Physiological and Molecular Responses Suggest Local Adaptation of the Lobe Coral *Porites lobata* to the Nearshore Environment

Kaho H Tisthammer*[a,b], Emma Timmins-Schiffman[c] , Francois O Seneca[a,d], Brook L Nunn[c] & Robert H Richmond[a]

a. Kewalo Marine Laboratory, University of Hawaii at Manoa, 41 Ahui Street, Honolulu, HI 96822 USA
b. (current address) Department of Biology, San Francisco State University, 1600 Holloway Avenue, San Francisco, CA 94132, USA
c. Department of Genome Sciences, University of Washington, Seattle, WA 98195, USA
d. (current address) Centre Scientifique de Monaco, 8, Quai Antoine 1er, 98000 Monaco

*Corresponding Author:
Kaho H Tisthammer, kahot@sfsu.edu

Keywords: corals, local adaptation, proteomics, reciprocal transplant experiment

ABSTRACT

Corals in nearshore marine environments are increasingly exposed to reduced water quality, which is the major local threat to coral reefs in Hawaii. Corals surviving in such conditions may have acclimatized and/or adapted to withstand sedimentation, pollutants, and other environmental stressors. Lobe coral (*Porites lobata*) populations from Maunalua Bay, Hawaii showed clear genetic differentiation along with distinct cellular protein expressions between the 'polluted, high-stress' nearshore site and the 'low-stress' offshore site. To understand the driving force of the observed genetic partitioning, reciprocal transplant and common-garden experiments were conducted using the nearshore and offshore colonies of *P. lobata* from Maunalua Bay to assess phenotypic differences of stress-related physiological and molecular responses between the two coral populations. Physiological responses (tissue layer thickness, tissue lipid content, and short-term growth rates) all showed differences between the populations, revealing more stress resilient traits in the nearshore corals. Proteomic responses highlighted the inherent differences in the cellular metabolic state and activities between the two populations under the same environmental conditions; nearshore corals did not significantly alter their proteome between the sites, while offshore corals responded to the nearshore transplantation with increased abundances of proteins associated with detoxification, antioxidant, and various metabolic processes. The response differences across multiple phenotypes suggest that the observed genetic partitioning was likely due to local adaptation of nearshore corals to the nearshore environmental conditions.

Significance Statement

Coral reefs are under serious threats from human activities, yet little is known about how corals respond and adapt to changing environments. Previous work from Hawaii shows corals living in 'nearshore' polluted areas are genetically differentiated from less-affected, yet nearby 'offshore' areas. Using these corals, we conducted a reciprocal transplant experiment to test a possibility of local adaptation. Shotgun proteomics was used to assess molecular responses, in addition to physiological responses. Clear differences in both responses were observed, and the results indicate more stress resilient traits and reduced responses to high-stress conditions in the nearshore corals. Together with the inherent differences in proteomic responses observed, our results suggest the nearshore corals are adapted to their habitat conditions.

INTRODUCTION

Coral reefs are among the most productive ecosystems on the planet, and are often called the rainforests of the ocean due to their complexity and biological diversity (1). Coral reefs provide important benefits to diverse species that inhabit them, and sustain the lives of hundreds of millions of people through their economic, cultural, physical, biological, recreational and ecological services (2). Coral reef ecosystems worldwide are, however, highly threatened by local and global stressors as a result of human activities, and coral cover around the world has declined over 50% in the past 100 years, (3-5). Rates of current environmental change are orders of magnitude faster than those of ice-age transitions (6), so the fate of coral reefs will ultimately depend on whether corals and their ecosystems can adequately adapt (genetically) or acclimatize (with physiological and ecological modifications) to such rapid environmental changes. Understanding coral's short-term adaptive ability is critical in order to accurately predict the future of coral reefs. Climate change, a global stressor that causes elevated sea surface temperature and changes in water chemistry, is viewed as the dominant threat to coral reefs. However, localized anthropogenic stressors, such as overfishing, pollution, and coastal development, also play significant roles in the decline of coral reefs (2, 7). Because coral reefs experiencing multiple stressors have a lower ecosystem resilience (4, 8-11), understanding the effects of local stressors and coral's adaptability to such stressors is vital as global level stressors continue to increase.

Nearshore marine habitats are increasingly exposed to reduced water quality due to human actions(12), and reduced water quality is one of the major local threats to coral reefs, especially in Hawaii. The health of coral reefs in Maunalua Bay, Oahu has drastically deteriorated due to large-scale urbanization that began in the last century(13). Corals in Maunalua Bay, especially in the nearshore areas, are under chronic stress from sedimentation and pollutant laden terrestrial runoff (14, 15). Despite prolonged exposure to these stressors, some individual corals continue to survive in the bay, suggesting these individuals may have acclimatized or adapted to withstand such stressors. A previously conducted physiological survey showed that the cellular stress responses in the lobe coral *Porites lobata* differed between colonies growing in the nearshore area exposed to reduced water quality and those from the relatively clean offshore area (Fig. 1). Population genetic analysis also revealed clear genetic differentiation between the nearshore and offshore populations in Maunalua Bay (16). Because the distance between the two sites is small (< 2 km) with no apparent barriers (17), the results suggest the possibility of local selection as the driving force of the observed genetic partitioning (16).

Based on these results, we tested whether the observed genetic differentiation between the nearshore and offshore populations of *P. lobata* in Maunalua Bay was due to local adaptation using reciprocal transplant and common garden experiments. *Porites lobata* in Maunalua Bay offers a unique opportunity to study the coral's adaptability at a population level since the environmental change and physical and chemical water properties at the bay have been well-documented and characterized. The species *P. lobata* also allows the assessment of the coral-host's adaptive abilities, as opposed to those of its endosymbiotic zooxanthellae, since *P. lobata* primarily harbors a specific clade of *Symbiodinium,* Clade C15 (18-21), which is vertically transmitted with high fidelity(21). To date, no shuffling of *Symbiodinium* in *P. lobata* has been reported. The goal of this study was to investigate how molecular and physiological responses differed between the two populations under the same environmental conditions, and to obtain any insight into the mechanisms involved in stress tolerance of corals to reduced water quality. Analyses of tissue layer thickness, tissue lipid content, and proteomic profiles of *P. lobata* were conducted following a 30-day reciprocal transplant experiment and short-term growth rates were compared using a common-garden experiment.

RESULTS

Physiological Response Differences between the Populations

Small fragments from five *P. lobata* source colonies from the two experimental sites, 'nearshore' and 'offshore', were used to conduct the 30-day reciprocal transplant experiment in the Maunalua Bay, Oahu, Hawaii (Fig. 1). The experimental results revealed clear physiological response differences between the two coral populations. The transplantation caused a significant reduction in the average tissue layer thickness in only one of the treatments; the offshore (O) corals transplanted to the nearshore (N) site (O→N corals) (Tukey HSD, $P < 0.001$, Fig. 2A, Table S1A). Contrary to the initial expectation that environmental stress might reduce the lipid content in corals, the total tissue lipid content in the offshore corals showed a marginally significant increase when transplanted to the nearshore site (Tukey HSD, $P = 0.078$), while nearshore corals showed very little change in their lipid content between the sites (Fig. 2B). Two-way ANOVA showed no population or transplant-site effects, but a significant interaction between the two factors (Table S1B). The short-term growth rates assessed using a common-garden experiment revealed a significantly higher average growth rate in the nearshore corals than the offshore corals. The nearshore corals grew on average 5.57% of their initial weight over 11 weeks, while the offshore corals grew 2.57% (Fig. 3, ANOVA, $F = 13.09$, $P = 0.0068$).

Proteomic Response: LC-MS/MS and protein identification

A label-free shotgun proteomics approach was performed to study the response differences in the coral proteomes between the two populations. The total number of LC-MS/MS runs (4 treatments [2 populations x 2 sites] x 3 biological replicates x 3 technical replicates = 36) identified a total of 3,635 proteins with high confidence (filtered at FDR of 0.01) based on the customized *P. lobata* protein database predicted from transcriptome (22). Of the total identified proteins, 487 proteins currently lack annotation. An average of 2,777 proteins were identified in each treatment (i.e. across the 3 biological replicates). A total of 1,977 proteins were shared across all four treatments, which likely represents the basic homeostatic functions of corals. Proteins unique to a treatment ranged from 105 to 233 (Table 1, Fig. S1).

The proteomic measurements were visualized using non-metric multidimensional scaling (NMDS) to evaluate the response differences among the treatments, using normalized spectral abundance factor (NSAF) values. After removing one outlier replicate from the dataset (one of the technical replicates of N→O corals [K17b]) , technical replicates were pooled to create one biological replicate in subsequent analyses. The NMDS analysis revealed a clear separation of the protein abundance profiles between the two populations regardless of the transplant sites (ANOSIM, R = 0. 7074, P = 0.004, Fig. S2). Transplantation appears to have had a greater effect on the offshore corals, while protein abundances of the nearshore corals were relatively similar between the transplant sites (discussed in more detail in the Response to cross transplantation section below).

Population specific protein abundance at each transplant site

A. Response differences at the nearshore site (N→N vs. O→N):

A total of 3,290 unique coral proteins were identified in N→N and O→N corals: 2,365 (72%) were shared between the two populations, leaving 402 proteins unique to N→N, and 523 unique to O→N corals. Gene Ontology (GO) enrichment analysis (metaGOmics P<0.01 cutoff, (23) identified 42 enriched GO terms unique to O→N corals from the three GO categories (Biological Process [BP], Molecular Function [MF], and Cellular Component [CC]), compared to N→N corals (Table S2). These included detoxification, antioxidant activity, lipid oxidation, intracellular protein transport, tricarboxylic acid (TCA) cycle, and purine-containing compound metabolic process. Only 19 unique terms were enriched in N→N corals, including peptidase inhibitor activity, oxidoreduction coenzyme metabolic process, lyase activity, and regulation of protein polymerization.

Our quantitative analysis on the proteomic data identified a total of 414 proteins to be differentially abundant between the two treatments, with 276 proteins significantly more abundant ('abundant proteins') in O→N corals, as opposed to 138 proteins more abundant in N→N corals (Dataset S1). GO analysis identified a total of 35 terms from the abundant proteins in O→N corals (Table S3, Fig. S3), while none met the statistical cutoff in N→N corals. The enriched terms in O→N corals indicated that the abundant proteins were dominated by those associated with amino acid metabolic process (tRNA aminoacylation), oxidation-reduction process, and vesicle membrane/coat. Visualization of all identified proteins and abundant protein datasets involved in metabolic pathways was conducted using iPath3(24). Similar to the GO analysis results, higher numbers of active metabolic and regulatory pathways were identified in O→N corals than N→N corals in all analyses (Fig. S4), including detoxification and glutathione pathways (*i.e.* antioxidant activity). The three most differentially abundant proteins with annotation in N→N corals relative to O→N corals were associated with immune function (m.9723: hemicentin-2, m.13233: Glycoprotein 340 (DMBT1), and m.12716: lectin MAL homologue), while those in O→N corals were involved with detoxification function (m.16246:arsenite methyltransferase, m.2139:E3 ubiquitin-protein ligase TRIM71, and m.16994:glutathione-S-transferase).

B. Response difference at the Offshore Site (N→O vs. O→O):

A total of 3,236 unique coral proteins were identified in N→O and O→O corals: 2,217 (68.5%) were shared between the two populations, leaving 656 proteins unique to N→O, and 363 unique to O→O corals. GO analysis identified 35 enriched GO terms unique in N→O

corals, compared to O→O corals, which involved amino acid biosynthetic process, ATP metabolic process, TCA cycles, fatty acid oxidation, and monosaccharide metabolic process. There were 15 unique GO terms in O→O corals, which included nucleotide monophosphate biosynthetic process, intracellular protein transport, vesicle organization, and GTP binding (Table S4).

Quantitative analysis indicated a total of 665 proteins to be significantly differentially abundant at the offshore site. N→O corals had 155 abundant proteins, and O→O corals had 510 abundant proteins. GO analysis resulted in identifying 35 enriched GO terms from abundant proteins in O→O corals, while only two GO terms met the cutoff value in N→O corals (Table S5). The enriched proteins in O→O corals were dominated by cellular functions related to protein translation (organonitrogen/nitrogen compound biosynthetic process and organic acid metabolic process, both leading to tRNA aminoacylation for protein translation, and tRNA aminoacyl ligase activity) and other catalytic activities (Fig. S5). Visualization of metabolic pathways by iPath2 using abundant proteins, as well as all identified proteins also highlighted the differences in the metabolic state between the nearshore and offshore corals under the same offshore environment (Fig. S6).

Response to cross transplantation

Effects of transplantation yielded a more diverse proteomic stress-response in the offshore corals than the nearshore corals (Fig. S2). The total number of significantly differentially abundant proteins between the sites was 135 for the nearshore corals (N→N *vs*. N→O), as opposed to 440 in the offshore corals (O→N *vs*. O→O). The number of unique GO terms identified between the sites was also higher in the offshore corals (69, Table S5) than in the nearshore corals (46, Table S6), reflecting the larger responses to cross transplantation in the offshore corals. Log fold changes of all identified proteins between the sites were significantly larger for the offshore corals than the nearshore corals (Wilcoxon Rank-Sum test, $P = 6.02 \cdot 10^{-9}$, Fig. S7). GO enrichment analysis indicated that the nearshore corals responded to transplantation to the offshore with increased amino acid biosynthesis, fatty acid beta oxidation, TCA cycle, chitin catabolism, coenzyme biosynthesis and translational initiation. The offshore corals responded to transplantation to the nearshore by increasing multiple metabolic processes (amino acid, fatty acid, ATP, monosaccharide, and carbohydrate derivative), detoxification, antioxidant activity, and protein complex subunit organization (Table 2). The shared responses between the transplanted corals (N→O and O→N) included increased fatty-acid beta oxidation, TCA cycle, carbohydrate derivative catabolic process, pyridoxal phosphate binding, and 'oxidoreductase activity acting on the CH-CH group of donors with flavin as acceptor', which likely represents the effects of transplantation to a non-native environment.

Proteome patterns across the four treatments

Comparing identified enriched GO terms across all treatments (Table 2) highlighted the unique state of O→N corals; a much higher number of 27 enriched GO terms were identified exclusively to O→N corals compared to the rest of the treatment (4 in O→O, 5 in N→N, and 15 in N→O). The most notable difference among the treatments was detoxification/antioxidant activity to be enriched exclusively in O→N corals. The number of proteins identified in this category was also the highest in O→N corals (27 vs. 20-23, Table 2).

Relative abundances of all proteins associated with select GO terms (P <0.01 in at least one treatment) were also compared across four treatments using the standardized NSAF values (Fig. 4). Hierarchical clustering of samples highlighted the larger difference between the populations than the transplant sites. Out of 26 BP terms compared, eight showed significant differences in their relative protein abundances among treatments (ANOVA, followed by Tukey HSD, Fig.4, Table S6), and eight out of 23 MF/CC terms showed significant differences among treatments. The comparison of protein abundances yielded mostly consistent results with GO analysis. For example, GO analysis indicated elevated 'fatty acid beta oxidation' in O→N corals, and relative abundance of proteins associated with the term was also higher in O→N corals. Similarly, 'TCA cycle' and 'mitochondrion' where the TCA cycle takes place were identified as enriched in O→N corals, and their associated protein abundances were also higher in O→N corals.

However, the relative abundance of proteins associated with detoxification ('detox proteins') was higher in the nearshore corals than the offshore corals when the NSAF values were aggregated for all detox proteins, even though elevated cellular detoxification activity was indicated exclusively in O→N corals by GO analysis (Fig. 5). Further examination of individual detox proteins revealed the following three points: 1) distinct sets of proteins were abundant in different treatments, rather than all detoxification proteins to be elevated in one treatment, and direction and magnitude of responses to transplantation were protein specific and varied between populations (Fig. 5). 2) Two peroxiredoxin (Prx) proteins, m.6147 (Prx-1) and m.9595 (Prx-6), dominated the relative abundance of detox proteins by having over an order of magnitude higher values. Also, they were in average 42% more abundant in the nearshore corals than the offshore corals (ANOVA, P = 0.00077), which resulted in overall higher abundance of detox proteins in the nearshore corals (ANOVA, P = 0.00226) (Fig. 4A). Without these two proteins, the aggregated relative abundance of detox proteins was higher in the offshore corals than the nearshore corals (ANOVA, P = 0.0421) (Table S7). 3) Some proteins with same or similar annotations had contrasting responses between the populations. For example, another Prx (m.17739, Prx4), which belongs to the same subfamily as Prx1, was significantly more abundant in the offshore corals (log2 fold change = 0.672, z-stat = 2.46). Similarly, m.17686 (peroxidasin homolog) was significantly more abundant in O→N corals (log2 fold change = 0.66, z-stat = 2.56), while m.9432 (peroxidasin homolog) was significantly more abundant in N→N corals (log2 fold change = 0.62, z-stat = 2.31), suggesting that the two populations potentially utilize different class/kind of enzymes as primary proteins in detoxification/antioxidant pathways.

To ascertain that the two proteins with same annotations are indeed different proteins, sequence similarity was compared for those that showed contrasting responses. The pairwise sequence identity of the two Prxs (m.6174 and m.17739) was 62.1 % for the overlapping 248 residues (Fig. S8A), and that of the two peroxidasins (m.9432 and m.17686) was 49.8% for the overlapping 442 residues (Fig. S8B), indicating that these two proteins are distinguishably different. The sequence similarity of all seven 'peroxidasin' like proteins identified in the detoxification category was only 21% (Supple. data 2), suggesting that corals possess multiple types of peroxidasin, and nearshore and offshore corals respond to stressors with different sets of peroxidasin. Hierarchical clustering of samples based on detox protein abundances (Fig. 5) again highlighted that coral protein responses were more similar between the populations than between the sites, and that the response to transplantation was in the offshore population.

Lastly, examining the GO terms unique to a pair of treatments identified that translation initiation factor activity was enriched at the offshore site in both populations (O→O, N→O), intracellular protein localization and purine nucleoside monophosphate biosynthetic process to be uniquely enriched in the offshore corals at both sites (O→O, O→N), and increased lyase activity in the nearshore corals at both sites (N→N, N→O).

DISCUSSION

Proteomic responses in corals have been previously studied (25, 26), but this is the first high throughput proteomic profile that allows rapid interrogation of the expression of thousands of proteins. Compared to previous coral protein studies, this approach identified an order of magnitude more protein identifications. Over 3,500 proteins were confidently identified from the 12 biological samples by matching tandem mass spectra to the protein database generated from *P. lobata* transcriptomes that contained >17,000 annotated protein sequences. The cnidarian relative *Nematostella* genome was estimated to contain ~18,000 protein-coding genes (27), and the scleractinian coral *Acropora digitifera* genome was reported to contain 23,668 predicted protein-coding loci (28). Thus, the protein database used in our analysis appears to represent a relatively thorough set of proteins in *P. lobata*. The genome of *P. lobata* is not yet available, and the number of proteins to be identified and annotated will likely increase once the genome becomes available, and proteomic data from ours and other studies will play a crucial role for accurate gene prediction and validation.

Resilient physiological traits in the nearshore corals

Physiological and molecular analyses of the nearshore and offshore coral populations exposed to the same environmental conditions revealed dynamic and divergent metabolic responses. This, together with clear genetic differentiation observed between the two populations (Tisthamemr et al. 2019) suggests that some inherent differences exist between the two populations although the effects of acclimatization cannot be ruled out completely. The response differences in tissue layer thickness (significant reduction in tissue layer thickness of O→ N corals) and short-term growth rate (lower growth rate in O corals) indicated that the nearshore corals possessed more resilient traits that responded to the environmental stressors. The tissue layer thickness of *Porites* corals is known to be reduced by sedimentation and other environmental stressors (29, 30). Between our experimental sites, sedimentation/turbidity was the most variable environmental parameter. For example, on average the mean turbidity varies by an order of magnitude between the sites (31), and high-turbidity events were more pronounced during and after storms at the nearshore site(13). Much lower light intensity recorded at the nearshore site during our experimental period also suggests higher turbidity there than the offshore site (Fig. S9). Therefore, the observed reduction in tissue layer thickness in O→N corals was likely due to sedimentation stress, which in turn reflects higher resilience of the nearshore corals to such a stressor. Faster growth rates observed in nearshore corals from the common-garden experiment in laboratory also suggest potential resilience to reduced water quality, since this experiment was conducted in conditions resembling the nearshore site. Seawater for the flow-through tank where the experiment was performed came from the Kewalo Channel, which receives several high volume terrestrial discharges, and boat-traffic based fuel contaminants. Additionally, the degree of daily temperature fluctuation of the experimental tank (2.97 ^{o}C daily max) mimicked nearshore site temperature variability (2.83 ^{o}C) more closely than offshore site variability (2.14 ^{o}C) (Fig. S8).

Increases in tissue lipid content observed in the cross-transplanted offshore corals (O→N corals) were unexpected, as decline in lipid is generally reported under stressful conditions(32-34). High sedimentation, however, has been observed to alter corals' metabolism by increasing the energy gains from heterotrophic sources (32, 35, 36). For example, when the coral *Stylohora subseriata* was transplanted to a eutrophic, nearshore site, their tissue lipid content increased, which was hypothesized to have resulted from an increase in both heterotrophic and phototrophic feeding (37). *Porites* species, however, show little evidence of having an ability to increase their heterotrophic feeding rate to meet their daily metabolic energy requirements. For example, < 10% of *Porites cylindrica*'s energy budget was met heterotrophically under a shaded condition (32), and *Porites compressa* and *P. lobata* did not increase their feeding rates after bleaching with significant loss of their lipid content, while *Montipora* species recovered their lipid content through feeding (38, 39). The increase in lipid content in the offshore corals was, therefore, not likely due to increased heterotrophic feeding. The difference could be due to differences in life history strategy between the two coral populations; investing in lipid storage *vs*. tissue growth under stressful conditions.

Comparing lipid contents before and after the experiment also revealed that lipid contents of the offshore corals increased significantly at both sites, while those of the nearshore corals did not (Fig. S10). Since lipid content can be affected by reproductive activities (oocyte production)(40) and the experiment took place during the pre-reproductive season, the lack of lipid increase in the nearshore corals may indicate their suppressed reproduction due to prolonged exposure to higher environmental stressors, making them so called "zombie" corals that appear healthy but do not reproduce (41). *Porites lobata* is a gonochoric spawner(42) and sexes of the source colonies could not be determined due to difficult nature involved in identifying sex in this species. Therefore, if there were more females in the offshore source colonies used in our experiment, this would explain the lipid increase seen after the experiment, but not the differences seen between the transplant sites. Still, little is known about intra- and interspecific variability, as well as seasonal changes in lipid content, specific sources of lipid carbon, and heterotrophic plasticity in corals. Available information suggests that lipid metabolism can differ substantially from species to species, and even from colony to colony (e.g. (32, 43, 44), which makes it difficult to draw a precise conclusion from our results. More studies will be necessary to uncover the reasons behind the observed phenomenon.

Reduced reaction in the nearshore corals to environmental stress

The proteomic response of the offshore corals at the nearshore site (O→N) was distinguishably different from the rest of the treatments. Elevated cellular stress responses, such as detoxification/antioxidant activity, along with increased metabolic activities were apparent in O→N corals from GO analysis, as well as higher total numbers of proteins detected in the corresponding GO categories. Increases in various metabolic processes suggest that O→N corals experienced a heightened demand for energy, due possibly to stress-mediated reactive oxygen species (ROS) production (45), and the energy demand appears to be met at least partially by a shift in energy metabolism, including β-oxidation of fatty acids(46), shown by the antioxidant activity and fatty acid beta-oxidation to be uniquely enriched in O→N corals with higher number and abundance of related proteins (Table 2, "Unique in O→N", Fig.4A).

The increased stress responses seen in the offshore corals at the 'high-stress' nearshore site indicates the reduced reaction of the nearshore corals to the same environment. The average fold changes in protein abundance in response to transplantation was significantly smaller in the nearshore corals than the offshore corals (Fig. S7). Additionally, the nearshore corals had the highest number of overlapping proteins (Fig. S11), and the lowest number of significantly differentially abundant proteins (Table S8) between the transplant sites. The physiological response results also followed the same trend as molecular responses, i.e. reduced reaction in the nearshore corals (Fig. 2), implying that the physiological stress level experienced by the nearshore corals was lower than that of the offshore corals. It is possible that such reduced responses may have resulted from residual effects of acclimatization of the nearshore corals to nearshore conditions. However, recent molecular studies suggest that scleractinian corals acclimate to new environmental conditions relatively quickly (in ~days), such as elevated temperature and pCO_2 (47, 48). Therefore, observed response differences between the two populations after a 30-day experimental period likely represent some fixed effects, i.e. adaptive evolution.

Potential molecular mechanism of stress resiliency

Proteomic responses unique to the nearshore corals, especially at the nearshore site, can shed light onto the potential mechanisms of stress resiliency of the nearshore corals to environmental stressors. Although no specific GO terms associated with the immune system processes were identified in the proteins from the nearshore corals, the most differentially abundant proteins in N→N corals (m.9723, m.13233 and m.12716) compared to O→N corals were related to immune responses. Certain environmental stressors, such as sedimentation and high temperature, can trigger or alter immune responses in corals (49, 50). Therefore, the nearshore corals' ability to upregulate these proteins or maintain them at high abundance (i.e. front-loading) may be contributing to their ability to thrive in the nearshore environments (51).

Peroxiredoxins (Prxs), which are detoxification proteins, are a ubiquitous family of thiol-specific antioxidant enzymes and often exist in high abundance with physiological importance (52, 53). Prx-like proteins were found in high abundance in *P. lobata* tissues, especially m.6174 (Prx1) and m.9595 (Prx6), which were over an order of magnitude higher compared to other proteins in the same GO category. Both proteins were also more abundant in the nearshore corals than the offshore corals at both sites (Table S7), suggesting that the stress resilient traits of the nearshore corals may stem from having naturally higher abundance of key redox proteins such as Prxs. Contrasting responses seen from the same or similar proteins indicate that the nearshore and offshore corals express and potentially possess different types and/or multiple sets of enzymes with similar functions to handle the same stressors. This functional redundancy may be characteristic of sessile organisms in high stress, intertidal environments. The sessile filter-feeder oyster *Crassostrea gigas* possesses extremely high number of heat shock proteins to combat the environmental stressors, compared to mobile, non-filter-feeding animals such as humans or mammal(54).

The cellular functions identified exclusively in the nearshore corals by GO analysis (Table 2) suggest that the nearshore corals had a higher level of 'oxidoreduction coenzyme metabolic process', which was also supported by the higher relative abundance of the proteins associated with this term, such as 3-hydroxyanthranilate 3,4-dioxygenase (m.19966), Fructose-

bisphosphate aldolase C (m.1369), and Nicotinamide mononucleotide adenylyltransferase 1 (m.9295) (Fig. 4). The metabolic pathway analysis results (Fig. S4A) indicated elevated sphingolipid metabolism in the nearshore corals. Sphingolipids are involved with many cellular physiological functions, such as regulation of cell growth, cell death, and differentiation (55), and recent studies have revealed much broader roles of its metabolites in signaling pathways associated with stress response, inflammation, apoptosis and autophagy (56, 57). Ceramide is one of the bioactive molecules in sphingolipid metabolism and has been identified as an important stress regulator, as many stressors result in ceramide accumulation, inducing apoptotic and cytotoxic responses, and ceramidases break down ceramide, preventing apoptosis and cell cycle arrest (56). One type of ceramidase (m.6024, acid ceramidase) was significantly more abundant in the nearshore corals (N→N) than the offshore corals (O→N and O→O), suggesting that the stress resilience of the nearshore corals may be related to their ability to better handle ceramide accumulation by increasing the ceramidase abundance. Ceramide also causes generation of reactive oxygen species, as well as the release of cytochrome *c* (58-60), which was consistent with the observed results of elevated antioxidant activity in the offshore corals (Table 2). Currently, 38 (27.5%) of the 138 significantly abundant proteins in the nearshore corals are unannotated or of unknown functions. Further investigation of the cellular pathways/functions related to these abundant proteins, especially with improved annotation, will help elucidate corals' mechanisms involved with stress tolerance.

Lastly, arsenite methyltransferase (m.16246) was one of the most differentially abundant proteins in O→N corals, compared to N→N corals. This enzyme methylates arsenite to form methylarsonate, which will be further converted to less toxic form for excretion. (Recent studies, however, suggest methylated intermediates and metabolites may be more reactive and toxic than inorganic arsenic, and thus this may not be simply a detoxification process (61, 62)). Arsenic contamination has been a concern for the nearshore environments in Oahu since arsenical compounds were used as pesticides on agricultural fields before the 1940s. Although no longer used, arsenic has remained in the soils, been continually transported into coastal waters, and bioaccumulated in marine macroalgae (63). Significantly more abundant arsenite methyltransferase in O→N corals compared to N→N corals, therefore, suggests higher sensitivity of the offshore corals to elevated arsenic exposure, (which in turn again indicates reduced responses of the nearshore corals to arsenic contaminants). The results also present a potential use of coral individuals that are not adapted to the nearshore conditions as a bioindicator of arsenic contamination in coastal waters.

CONCLUSIONS

At Maunalua Bay, Hawaii, a steep environmental gradient exists from the mouth of the bay toward offshore in a relatively short distance (~2 km), and the corals living in such contrasting environment of 'high-stress' nearshore and 'less-stress' offshore sites are genetically differentiated. The reciprocal transplant and common-garden experimental results highlighted phenotypic differences in stress responses between these nearshore and offshore coral populations. The physiological traits indicated more stress resilient traits of the nearshore corals to reduced water quality. Proteomic responses revealed fixed differences in the metabolic state between these corals, as well as reduced responses of the nearshore corals to environmental stressors. The results also provided insight into molecular mechanisms of stress resiliency in

corals. The response differences across multiple phenotypes suggest that the deteriorated water and substrate quality in the nearshore environment have likely subjected the nearshore corals to selection, causing local adaptation, since anthropogenic stressors, such as sedimentation and pollution can facilitate local adaptation of the nearshore marine organisms (64, 65). However, nearshore marine habitats naturally experience higher fluctuations in temperature and other environmental variables, and this unique environmental niche may be occupied by select certain genotypes that could better tolerate such environmental fluctuations. Further studies are needed to understand the true force behind the observed phenotypic and genetic differences between the sites. For conservation, our study results highlight the importance of protecting corals surviving in the marginal habitats, as they may possess more stress tolerant traits, and could seed the future coral reefs under rapidly changing environments with increasing stressors.

MATERIALS AND METHODS

Sample Collection and Reciprocal Transplant Experiment

Five individual *P. lobata* colonies were selected as source colonies from the nearshore and offshore sites for the reciprocal transplant experiment. All samples were identified as *P. lobata* through colony morphology, corallite skeletal morphology (66), and DNA analysis of Histone2 (H2) marker (Table S9, Tisthammer et al, 2019). Ten small fragments (approximately 1.5 cm in diameter) from each source colony were collected from the upward facing surface on April 15, 2015. One sample was immediately frozen on shore using liquid nitrogen and another was fixed in 10% Z-fix in filtered seawater for baseline data. Half of the remaining coral fragments from each colony were cross-transplanted to the other location, and the remaining half were back-transplanted to their original location for 30 days (Fig. 1B). Temperature profiles were measured by deploying a data logger (HOBO®, Onset Computer, Bourne, MA) at each site. Extensive chemical and physical data of Maunalua Bay's sediments and water were referenced from previous studies(17, 31, 67). At the end of the experiment, one fragment of each source colony at each location was flash frozen on site using liquid nitrogen and stored at -80℃ at the Kewalo Marine Laboratory (KML), University of Hawaii at Manoa, for protein analyses. The other source colony fragments were fixed in Z-fix for physiological assays.

Tissue Layer Thickness & Tissue Lipid Content Assessment

The coral fragments preserved in Z-fix were rinsed with distilled water and dried at room-temperature overnight. All coral fragments were then cut in half vertically, and the thickness of the exposed tissue layer was measured to the nearest 0.01 mm using a digital caliper. Ten measurements were taken from each specimen, to account for the variability within a sample, and the results were analyzed using nested 2-way, followed by Tukey HSD post hoc test.

The dried coral fragments were used to analyze the total tissue lipid content of holobionts using the modified method of Stimson (1987). The dried samples were first decalcified in ~10% hydrochloric acid. The decalcified samples were then rinsed with distilled water, and placed in 50 mL polypropylene centrifuge tubes containing an adequate volume of chloroform-methanol (2:1) for over 24 hours for lipid extraction. The solvent-extract solution was decanted into a pre-weighed glass beaker through a coarse paper filter, and the filter and remaining tissues were rinsed with additional fresh chloroform-methanol solvent. The solvent was evaporated at 55°C, and the remaining extracts were weighted to the nearest 0.1 mg. The remaining tissues were

dried completely at room temperature and weighed to the nearest 0.1 mg. The total lipid content is expressed as percent lipid per dried tissue (w/w). The results were compared among treatments using 2-way ANOVA, followed by Tukey HSD test, as in the tissue layer thickness results.

Proteomic Analysis

The same three individuals from each site were selected for proteomic analysis (3 indiv. x 4 treatments = 12 total samples). The frozen coral fragments were pulverized using a chilled mortar and a pestle with liquid nitrogen, and coral proteins (the S9 post-mitochondrial fraction of coral host protein) were extracted and quantified using the bicinchoninic acid (BCA) assay as described in (68) with modifications. Briefly, proteins were homogenized in 6M urea in 50mM ammonium bicarbonate in a microtube using Tissue-Tearor™ (BioSpec Products Inc) on ice. The homogenate was centrifuged at 10,000 rcf for > 20 minutes at 4℃ to eliminate the zooxanthellae, and the collected supernatant was quantified by the BCA assay, and stored at -80 ℃. An equal quantity (80 µg) of protein was placed in an Eppendorf® LoBind microcentrifuge tube with a total of 100 µl of 6M urea in 50mM ammonium bicarbonate. The protein samples were alkylated and digested with trypsin (Pierce™ Trypsin Protease MS-Grade) with 1:20 (w/w) enzyme to protein ratio for overnight at room temperature, following the protocol of (69) with modification.

Peptide samples were analyzed in triplicate on the Thermo Scientific Q- Exactive tandem mass spectrometer using data dependent analysis with the top 20 ions selected for MS2 analysis. Peptides entering the mass spectrometer were separated using liquid chromatography (5-35% acetonitrile over 90 minutes) on a 3 cm pre-column and 30 cm analytical column, both packed with 3 µm C18 beads (Dr. Maisch). [Need to include database searches with Comet and TPP]. Normalized spectral abundance factor (NSAF) for consensus protein inferences was calculated in Abacus (70). Differentially abundant proteins were determined using QSpec (71). Non-metric multidimensional scaling analysis was conducted on the square-root transformed NSAF values with Wisconsin double standardization, and based on a Bray-Curtis dissimilarity matrix in the *vegan* package (72) in R v. 3.4.0 (R Core Team). Statistically significant separations among samples based on treatment (nearshore vs. offshore corals, as well as each treatment) were calculated using ANOSIM in *vegan* based on 5000 permutations (R = 0. 7074, P = 0.004, and R = 0.5864, P = 0.0002).

Common Garden Experiment

Live coral fragments from five source colonies were collected from the nearshore and offshore sites in Maunalua Bay, and divided into six small nubbins of approximately 2 cm^2 per sample. All nubbins were glued to a ceramic tile with marine epoxy with an identification tag, and placed in an outdoor flow-through seawater tank at KML with a temperature logger. After three weeks of healing time, the buoyant weighing method was used to determine the short term growth rate; each coral nubbin was measured weekly for 11 weeks to the nearest 0.01g using a digital scale (Ohaus SPX222, Parsippany, NJ). The coral nubbins were placed randomly in the tank every week to eliminate the tank effect. The average percent gain of five individuals relative to their initial weights was log transformed and analyzed using ANOVA.

ACKNOWLEDGEMENTS

We thank V. Sindorf for field assistance. Special thanks to J. Martinez and T. Oliver for their support and advice. Coral samples were collected under the Hawaii Division of Aquatic

Resources, Special Activity Permit 2015-06. Financial support came from the National Fish and Wildlife Foundation (Grant Number 34413), the Hawaii Department of Health (MOA 13-502), and the NOAA Coral Reef Ecosystem Studies Program (NA09NOS4780178).

REFERENCES

1. Reaka-Kudla ML (1997) The Global Biodiversity of Coral Reefs: A Comparison with Rain Forests. *Biodiversity II: Understanding and Protecting Our Biological Resources*, eds Wilson EO, Wilson DE, Reaka-Kudla ML (Joseph Henry Press, Washington, D.C.), pp 83–108.
2. Aswani S, et al. (2015) Scientific frontiers in the management of coral reefs. *Frontiers in Marine Science* 2:50.
3. Hughes TP, Graham NAJ, Jackson JBC, Mumby PJ, Steneck RS (2010) Rising to the challenge of sustaining coral reef resilience. *TRENDS in Ecology and Evolution* 25(11):633–642.
4. Richmond RH, Wolanski E (2011) Coral research: past efforts and future horizons. *Corals Reefs an Ecosystem in Transition*, eds Dubinsky Z, Stambler N (Springer, Dordrecht), pp 3–12.
5. Graham NAJ (2014) Habitat Complexity: Coral Structural Loss Leads to Fisheries Declines. *Current Biology* 24(9):R359–R361.
6. Hoegh-Guldberg O, et al. (2007) Coral Reefs Under Rapid Climate Change and Ocean Acidification. *Science* 318(5857):1737–1742.
7. Morgan KM, Perry CT, Smithers SG, Johnson JA, Daniell JJ (2016) Evidence of extensive reef development and high coral cover in nearshore environments: implications for understanding coral adaptation in turbid settings. *Sci Rep* 6:29616.
8. West JM, Salm RV (2003) Resistance and resilience to coral bleaching: implications for coral reef conservation and management. *Conservation Biology* 17(4):956–967.
9. Carilli JE, Norris RD, Black BA, Walsh SM, McField M (2009) Local stressors reduce coral resilience to bleaching. *PLoS ONE* 4(7):e6324.
10. Kennedy EV, et al. (2013) Avoiding coral reef functional collapse requires local and global action. *Current Biology* 23(10):912–918.
11. Ban SS, Graham NAJ, Connolly SR (2014) Evidence for multiple stressor interactions and effects on coral reefs. *Global Change Biology* 20(3):681–697.
12. Wenger AS, et al. (2016) Effects of reduced water quality on coral reefs in and out of no-take marine reserves. *Conservation Biology* 20(1):142–153.
13. Wolanski E, Martinez JA, Richmond RH (2009) Quantifying the impact of watershed urbanization on a coral reef: Maunalua Bay, Hawaii. *Estuarine, Coastal and Shelf Science* 84(2):259–268.
14. Richmond RH (2011) *HCRI Project Report (FY2009-2010): Watersheds impacts on coral reefs in Maunalua Bay, Oahu, Hawaii* (Hawaii Coral Reef Initiatives).
15. Richmond RH (2008) *HCRI Project Final Report (FY 2007): Watersheds impacts on Maunalua Bay, Oahu, Hawaii* (Hawaii Coral Reef Initiatives).
16. Tisthammer KH, Forsman ZH, Richmond RH (2018) Isolation by adaptation? Genetic structure is stronger across habitats than islands in the coral *Porites lobata* from Oahu and Maui. *PLosOne (in revision)*.
17. Presto KM, Storlazzi CD, Logan JB, Reiss TE, Rosenberger KJ (2012) *Coastal*

Circulation and Potential Coral-larval Dispersal in Maunalua Bay, Oahu, Hawaii - Measurements of waves, Currents, Temperature, and salinity June-September 2010 (U.S. Geological Survey Open-File Report 2012-1040).
18. LaJeunesse T, et al. (2004) High diversity and host specificity observed among symbiotic dinoflagellates in reef coral communities from Hawaii. *Coral Reefs* 23:596–603.
19. Smith LW, Wirshing HH, Baker AC, Birkeland C (2008) Environmental versus genetic influences on growth rates of the corals Pocillopora eydouxi and Porites lobata (Anthozoa: Scleractinia) 1. *Pacific Science* 62(1):57–69.
20. Barshis DJ, et al. (2010) Protein expression and genetic structure of the coral *Porites lobata* in an environmentally extreme Samoan back reef: does host genotype limit phenotypic plasticity? *Molecular Ecology* 19(8):140297–140297.
21. Fabina NS, Putnam HM, Franklin EC, Stat M, Gates RD (2012) Transmission mode predicts specificity and interaction patterns in coral-*Symbiodinium* networks. *PLoS ONE* 7(9):e44970.
22. Bhattacharya D, et al. (2016) Comparative genomics explains the evolutionary success of reef-forming corals. *Elife* 5:5741.
23. Riffle M, et al. (2018) MetaGOmics: A Web-Based Tool for Peptide-Centric Functional and Taxonomic Analysis of Metaproteomics Data. *Proteomes* 6(1):2–17.
24. Darzi Y, Letunic I, Bork P, Yamada T (2018) iPath3.0: interactive pathways explorer v3. *Nucleic Acids Research* 46(W1):W510–W513.
25. Weston AJ, et al. (2015) Proteomics links the redox state to calcium signaling during bleaching of the scleractinian coral *Acropora microphthalma* on exposure to high solar Irradiance and thermal stress. *Molecular & Cellular Proteomics* 14(3):585–595.
26. Garcia GD, et al. (2016) Metaproteomics reveals metabolic transitions between healthy and diseased stony coral Mussismilia braziliensis. *Molecular Ecology* 25(18):4632–4644.
27. Putnam NH, et al. (2007) Sea anemone genome reveals ancestral eumetazoan gene repertoire and genomic organization. *Science* 317:86–94.
28. Shinzato C, et al. (2012) Using the Acropora digitifera genome to understand coral responses to environmental change. *Nature* 476(7360):320–323.
29. Barnes DJ, Lough JM (1999) Porites growth characteristics in a changed environment: Misima Island, Papua New Guinea. *Coral Reefs* 18(3):213–218.
30. Rotmann S, Thomas S (2012) Coral Tissue Thickness as a Bioindicator of Mine-Related Turbidity Stress on Coral Reefs at Lihir Island, Papua New Guinea. *Oceanography* 25(4):52–63.
31. Storlazzi CD, Presto KM, Logan JB, Field ME (2010) *Coastal Circulation and Sediment Dynamics in Maunalua Bay, Oahu, Hawaii* (USGS Open-File Report 2010-1217).
32. Anthony K, Fabricius K (2000) Shifting roles of heterotrophy and autotrophy in coral energetics under varying turbidity. *Journal of Experimental Marine Biology and Ecology* 252(2):221–253.
33. Yamashiro H, Oku H, Onaga K (2005) Effect of bleaching on lipid content and composition of Okinawan corals. *Fisheries Science* 71(2):448–453.
34. Anthony K, Connolly SR, Hoegh-Guldberg O (2007) Bleaching, energetics, and coral mortality risk: Effects of temperature, light, and sediment regime. *Limnology and Oceanography* 52(2):716–726.
35. Fabricius KE (2005) Effects of terrestrial runoff on the ecology of corals and coral reefs: review and synthesis. *Marine Pollution Bulletin* 50(2):125–146.

36. Baumann J, Grottoli AG, Hughes AD, Matsui Y (2014) Photoautotrophic and heterotrophic carbon in bleached and non-bleached coral lipid acquisition and storage. *Journal of Experimental Marine Biology and Ecology* 461:469–478.
37. Seemann J, Sawall Y, Auel H, Richter C (2012) The Use of Lipids and Fatty Acids to Measure the Trophic Plasticity of the Coral Stylophora subseriata. *Lipids* 48(3):275–286.
38. Grottoli AG, Rodrigues LJ, Juarez C (2004) Lipids and stable carbon isotopes in two species of Hawaiian corals, Porites compressa and Montipora verrucosa, following a bleaching event. *Marine Biology* 145(3):621–631.
39. Grottoli AG, Rodrigues LJ, Palardy JE (2006) Heterotrophic plasticity and resilience in bleached corals. *Nature* 440(7088):1186–1189.
40. Oku H, Yamashiro H, Onaga K, Sakai K, Iwasaki H (2003) Seasonal changes in the content and composition of lipids in the coral *Goniastrea aspera*. *Coral Reefs* 22:83–85.
41. Watson R, Howell B (2013) VI. Closing the Coral Commons to Support Reef Restoration in Florida. *Conservation Leadership Council*.
42. Richmond RH, Hunter CL (1990) Reproduction and recruitment of corals: Comparisons among the Caribbean, the Tropical Pacific, and the Red Sea. *Marine ecology Progress Series* 60(1):185–203.
43. Teece MA, Estes B, Gelsleichter E, Lirman D (2011) Heterotrophic and autotrophic assimilation of fatty acids by two scleractinian corals, Montastraea faveolataand Porites astreoides. *Limnology and Oceanography* 56(4):1285–1296.
44. Hinrichs S, et al. (2013) Seasonal variations in energy levels and metabolic processes of two dominant Acropora species (A. spicifera and A. digitifera) at Ningaloo Reef. *Coral Reefs* 32(3):623–635.
45. Ray PD, Huang B-W, Tsuji Y (2012) Reactive oxygen species (ROS) homeostasis and redox regulation in cellular signaling. *Cellular Signalling* 24(5):981–990.
46. Tomanek L (2014) Proteomics to study adaptations in marine organisms to environmental stress. *Journal of Proteomics* 105(C):92–106.
47. Bay RA, Palumbi SR (2015) Rapid Acclimation Ability Mediated by Transcriptome Changes in Reef-Building Corals. *Genome Biology and Evolution* 7(6):1602–1612.
48. Moya A, et al. (2015) Rapid acclimation of juvenile corals to CO 2-mediated acidification by upregulation of heat shock protein and Bcl-2 genes. *Molecular Ecology* 24(2):438–452.
49. Sheridan C, Grosjean P, Leblud J, Palmer CV (2014) Sedimentation rapidly induces an immune response and depletes energy stores in a hard coral. *Coral Reefs*. doi:10.1007/s00338-014-1202-x.
50. Pinzón JH, et al. (2015) Whole transcriptome analysis reveals changes in expression of immune-related genes during and after bleaching in a reef-building coral. *Royal Society Open Science* 2(4):140214–140214.
51. Barshis DJ, et al. (2013) Genomic basis for coral resilience to climate change. *Proc Natl Acad Sci USA* 110(4):1387–1392.
52. Tairum CA Jr, de Oliveira MA, Horta BB, Zara FJ, Netto LES (2012) Disulfide Biochemistry in 2-Cys Peroxiredoxin: Requirement of Glu50 and Arg146 for the Reduction of Yeast Tsa1 by Thioredoxin. *Journal of Molecular Biology* 424(1-2):28–41.
53. Perkins A, Nelson KJ, Parsonage D, Poole LB, Karplus PA (2015) Peroxiredoxins: guardians against oxidative stress and modulators of peroxide signaling. *Trends in Biochemical Sciences* 40(8):435–445.
54. Zhang G, et al. (2012) The oyster genome reveals stress adaptation and complexity of

shell formation. *Nature* 490(7418):49–54.
55. Spiegel S, Merrill AH (1996) Sphingolipid metabolism and cell growth regulation. *FASEB J* 10(12):1388–1397.
56. Hannun YA, Obeid LM (2002) The Ceramide-centric Universe of Lipid-mediated Cell Regulation: Stress Encounters of the Lipid Kind. *Journal of Biological Chemistry* 277(29):25847–25850.
57. Pralhada Rao R, et al. (2013) Sphingolipid Metabolic Pathway: An Overview of Major Roles Played in Human Diseases. *Journal of Lipids* 2013(14):1–12.
58. García-Ruiz C, Colell A, Marí M, Morales A, Fernández-Checa JC (1997) Direct effect of ceramide on the mitochondrial electron transport chain leads to generation of reactive oxygen species. Role of mitochondrial glutathione. *Journal of Biological Chemistry* 272(17):11369–11377.
59. Ghafourifar P, et al. (1999) Ceramide induces cytochrome c release from isolated mitochondria Importance of mitochondrial redox state. *Journal of Biological Chemistry* 274(10):6080–6084.
60. Corda S, Laplace C, Vicaut E, Duranteau J (2001) Rapid reactive oxygen species production by mitochondria in endothelial cells exposed to tumor necrosis factor-alpha is mediated by ceramide. *Am J Respir Cell Mol Biol* 24(6):762–768.
61. THOMAS D, Waters SB, Styblo M (2004) Elucidating the pathway for arsenic methylation*1. *Toxicology and Applied Pharmacology* 198(3):319–326.
62. Thomas DJ, et al. (2007) Arsenic (+3 oxidation state) methyltransferase and the methylation of arsenicals. *Exp Biol Med (Maywood)* 232(1):3–13.
63. USGS (2012) *Water Resources Research Center Annual Technical Report FY 2012* (The State Water Resources Research Institute Program, USGS).
64. Puritz JB, Toonen RJ (2011) Coastal pollution limits pelagic larval dispersal. *Nature Commnications* 2:226.
65. Sanford E, Kelly MW (2011) Local Adaptation in Marine Invertebrates. *Annu Rev Marine Sci* 3(1):509–535.
66. Tisthammer KH, Richmond RH (2018) Corallite skeletal morphological variation in Hawaiian Porites lobata. *Coral Reefs* 65:560–14.
67. Richmond RH (2009) *HCRI Project Progress Report FY2008: Watersheds impacts on coral reefs in Maunalua Bay, Oahu, Hawaii*.
68. Murphy JWA, Richmond RH (2016) Changes to coral health and metabolic activity under oxygen deprivation. *PeerJ* 4(2):e1956.
69. Nunn BL, Slattery KV, Cameron KA, Timmins-Schiffman E, Junge K (2015) Proteomics of Colwellia psychrerythraeaat subzero temperatures - a life with limited movement, flexible membranes and vital DNA repair. *Environmental Microbiology* 17(7):2319–2335.
70. Fermin D, Basrur V, Yocum AK, Nesvizhskii AI (2011) Abacus: A computational tool for extracting and pre-processing spectral count data for label-free quantitative proteomic analysis. *Proteomics* 11(7):1340–1345.
71. Choi H, Kim S, Fermin D, Tsou C-C, Nesvizhskii AI (2015) Journal of Proteomics. *Journal of Proteomics* 129(C):121–126.
72. Okansen J, et al. (2013) Package “vegan” : Community Ecology Package, R package version 2.0-10. 1–263.

Figure 1. Map of study locations (A) and a diagram of the reciprocal transplant experimental design (B).

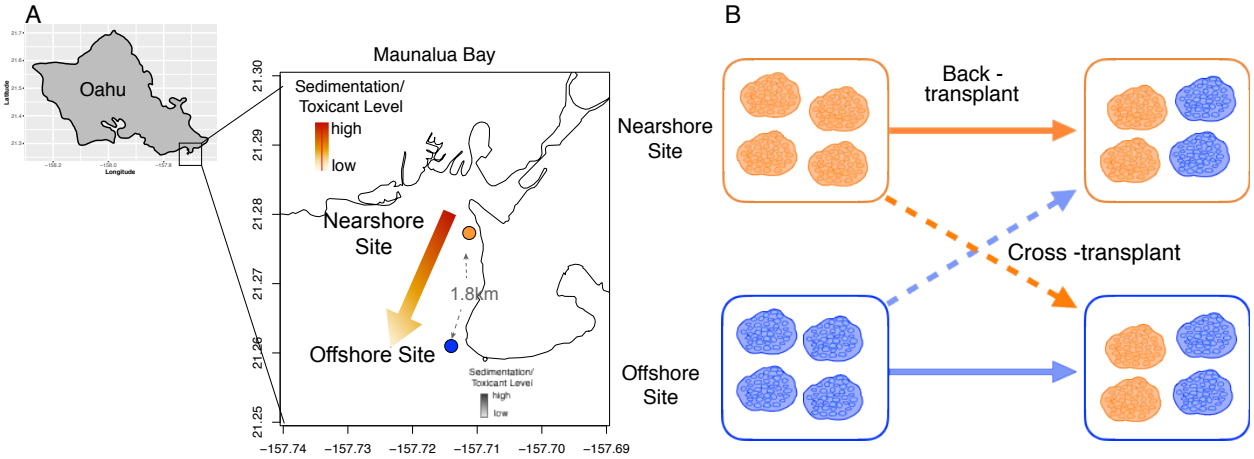

Figure 2. Results of the 30-day reciprocal transplant experiment I: A) Tissue layer thickness (mm) measurements of *P. lobata*, and B) tissue lipid content (%) of *P. lobata* holobiont. Arrows show the direction of transplanting. Different letters indicate a statistically significant difference.

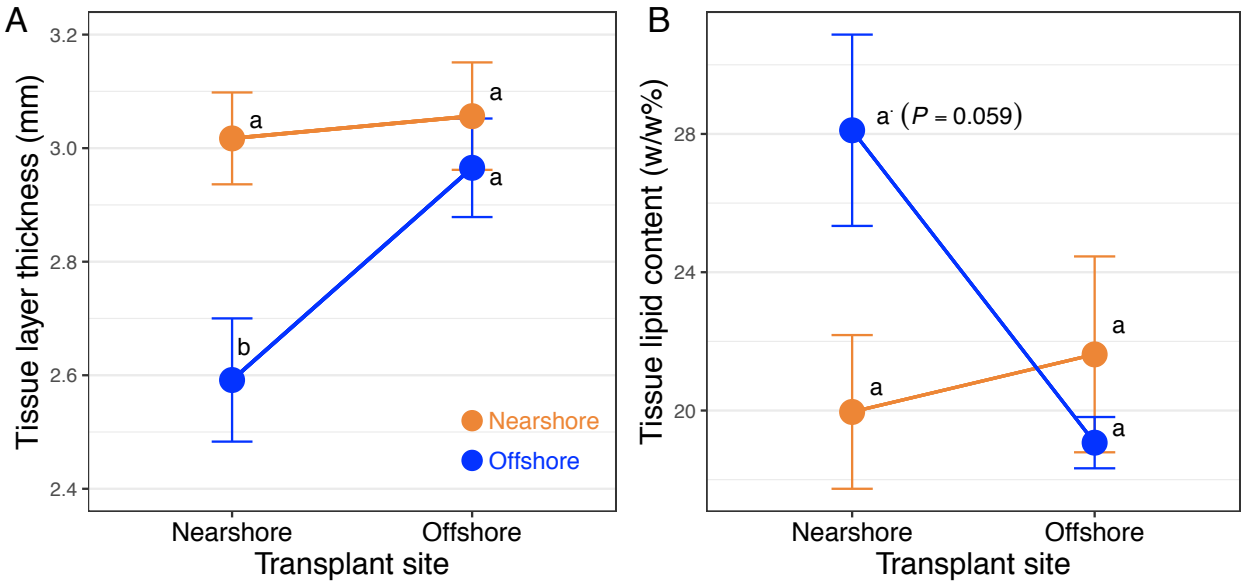

Figure 3. Short-term growth rate of two genotypes of *P. lobata* in a common-garden setting. The error bars denote standard error.

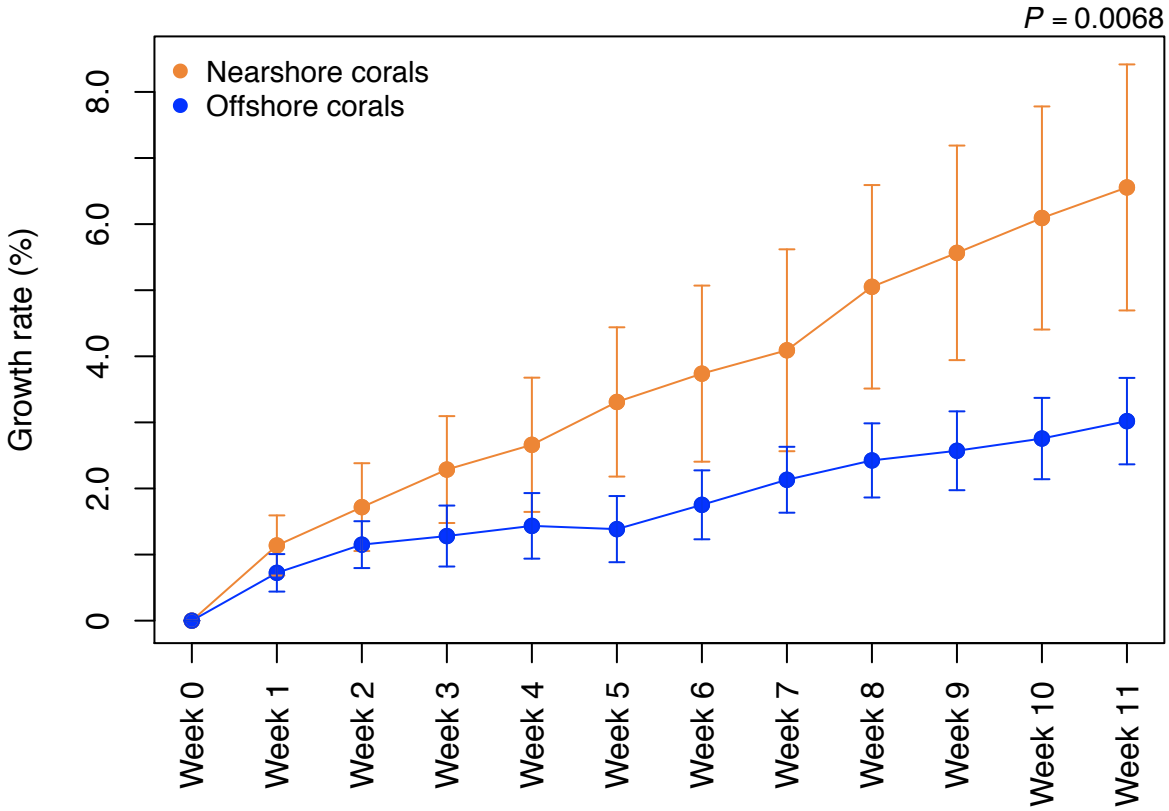

Figure 4. Comparison of relative protein abundance based on the total NSAF values of proteins belonging to each GO term. Hierarchical clustering was conducted in gplots using R. A: Biological Process terms. B: Molecular Function and Cellular Component terms. The numbers next to the GO terms indicate statistically significant differences in adjusted NSAF values between a pair of treatment (anova, followed by TukeyHSD): 1=N→N *vs*. O→N , 2=N→N *vs*. N→O, 3=N→N *vs*. O→O, 4=N→O *vs*. O→N, 5=O→O *vs*. O→N, 6=O→O *vs*. N→O

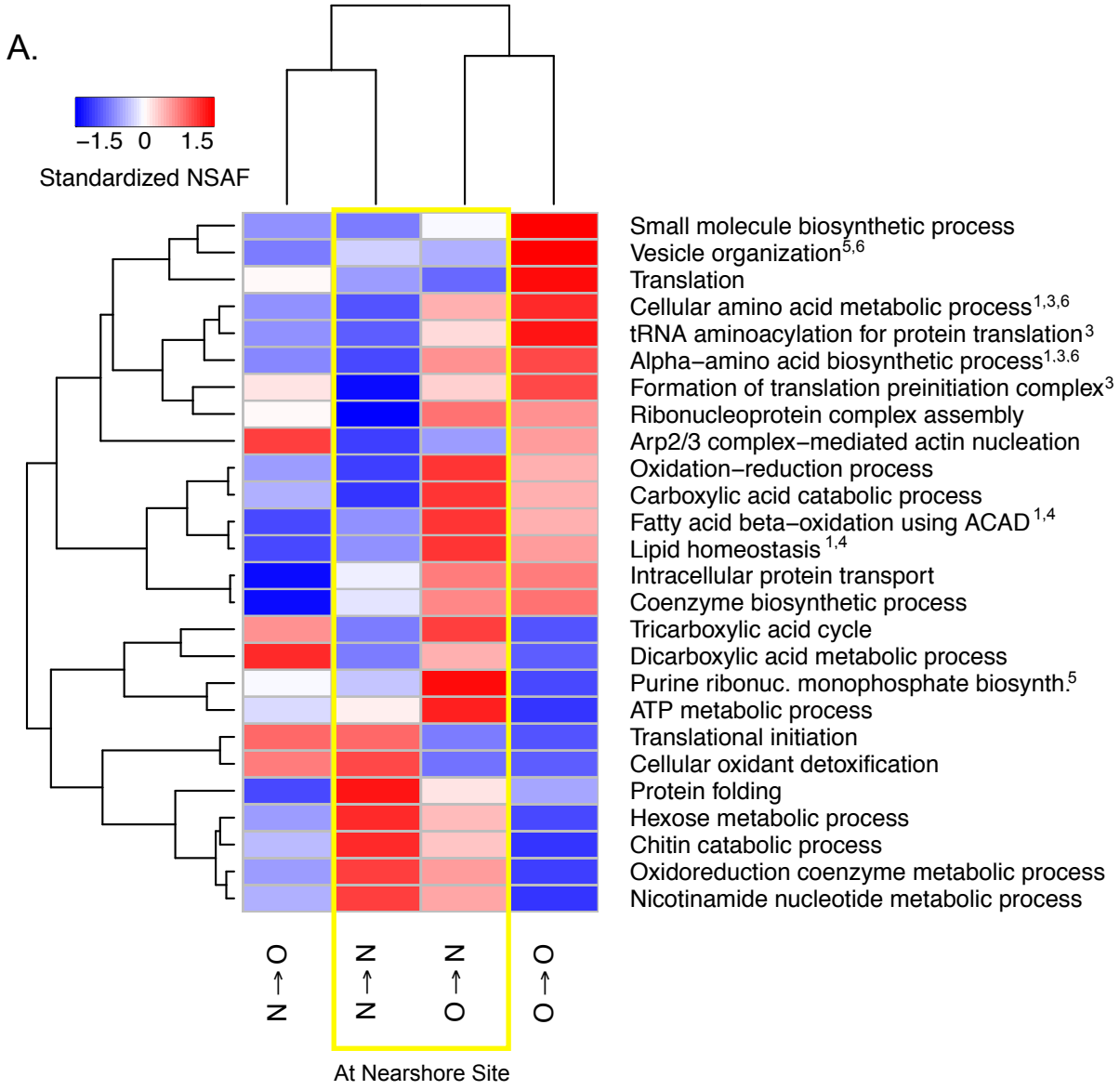

B.

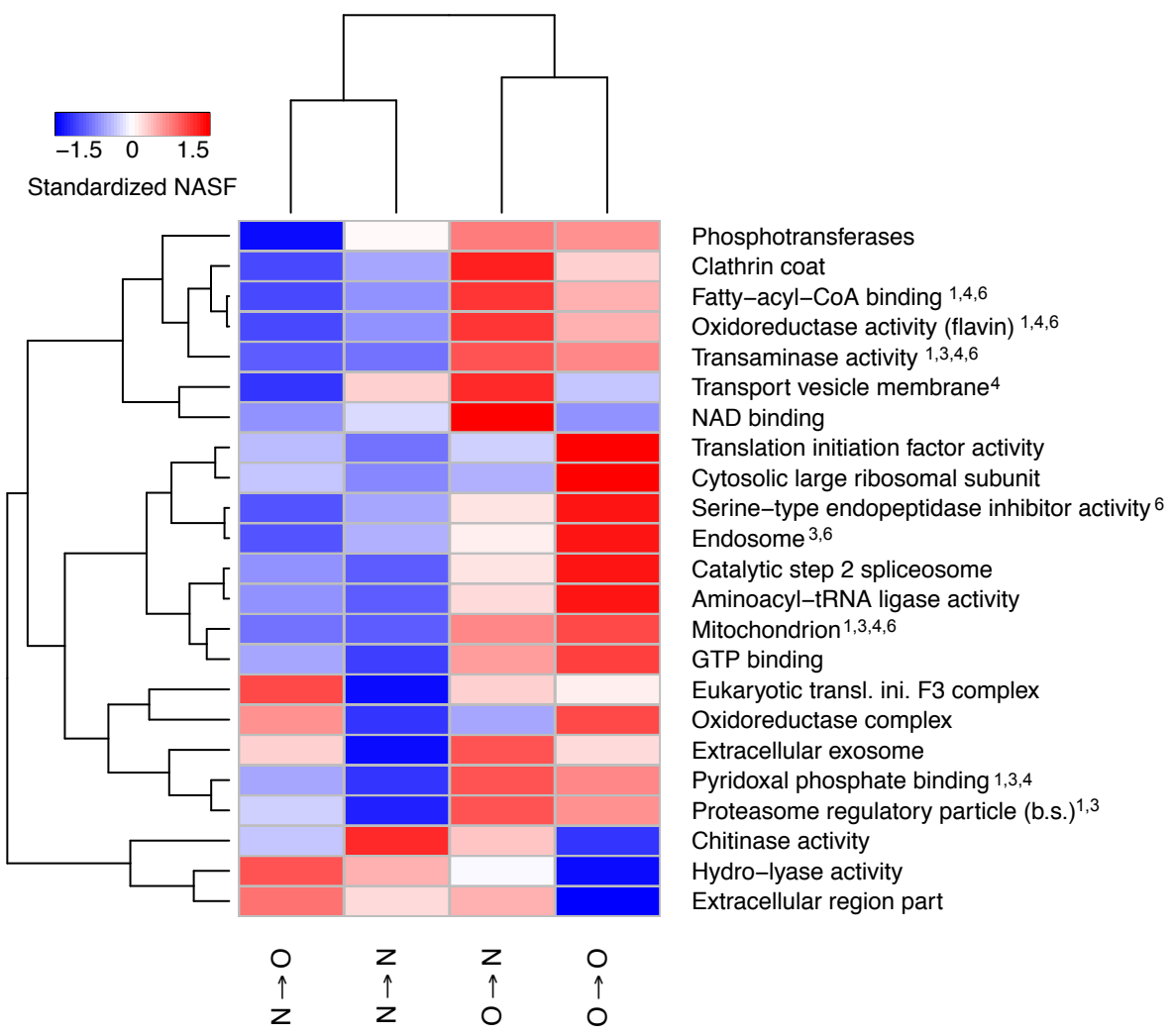

b.s.= base complex

Figure 5 Responses of detoxification proteins of *P. lobata* following a 30-day reciprocal transplant experiment. * denotes statistically significantly differences in protein abundance between N→N and O→N corals by Qspec. Contrasting responses observed between the nearshore and offshore corals discussed are highlighted (Peroxiredoxins in blue, and peroxidasin homologs in yellow).

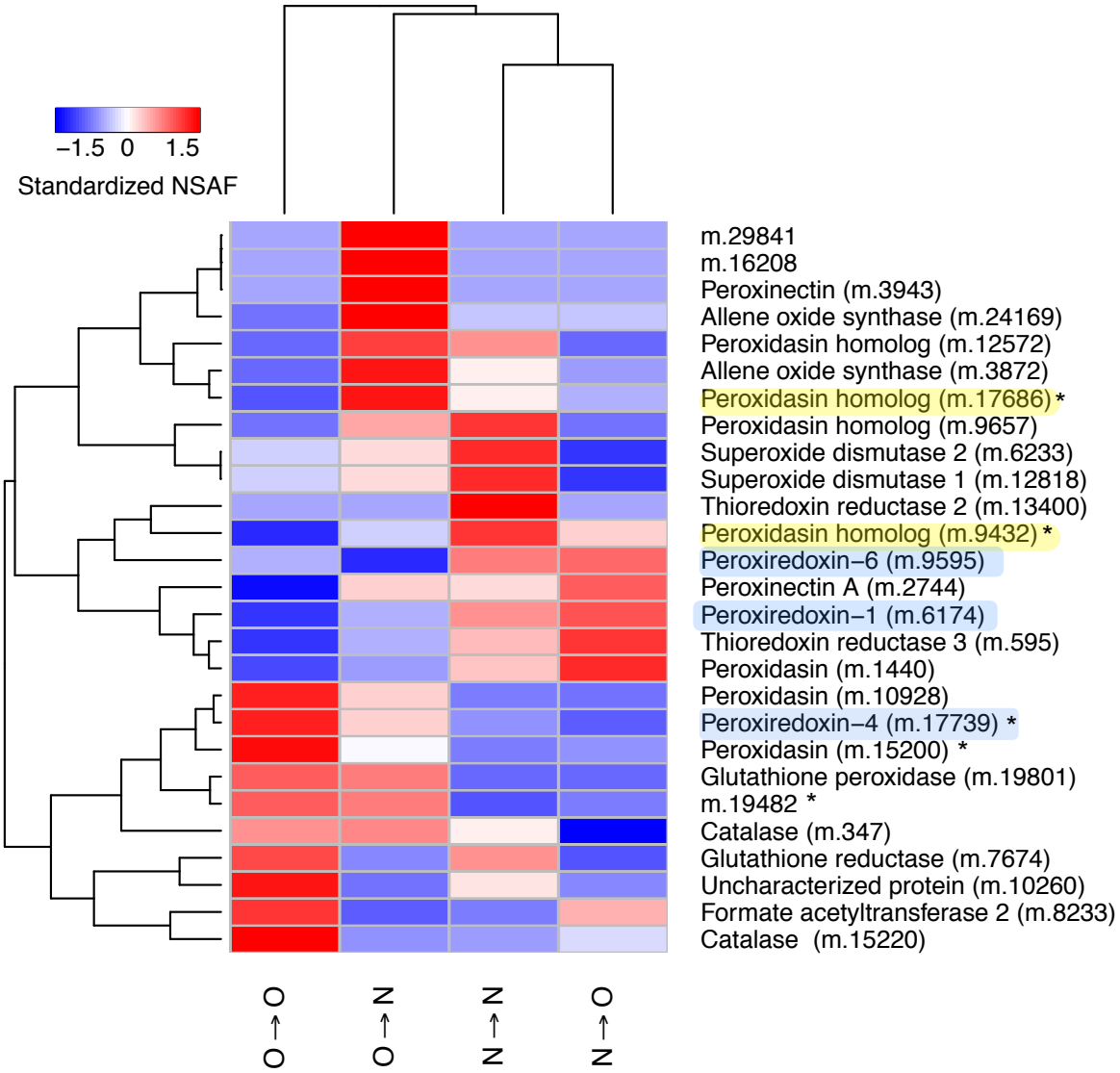

Table 1. Summary statistics of the numbers of proteins and associated Gene Ontology (GO) terms identified in the samples from each treatment. N=Nearshore corals, O= Offshore corals.

treatment	Nearshore Site		Offshore Site		Ave.	Total
	N (N→N)	O (O→N)	N (N→O)	O (O→O)		
No. of coral proteins identified	2767	2888	2873	2580	2777	3635
No. of annotated proteins	2475	2621	2497	2262	2464	3246
No. of proteins unique to a treatment	105	233	157	142	159	-
No. of GO terms identified	163	186	185	165	175	233
No. of GO terms unique to a treatment	4	26	13	6	12	-

Table 2. The enriched GO terms uniquely identified in one or two of the treatments. The identified cellular pathways/functions are grouped starting with the most parent term. Functions are listed starting with a group with the most GO terms, and then in order of P-value. BP = Biological Process, MF = Molecular Function, and CC= Cellular Component of the GO categories.

GO Terms	GO Cat.	P-values				No. of Proteins			
		NN	ON	OO	NO	NN	ON	OO	NO
Offshore Site (N→O, O→O)									
1. translational initiation	BP	2.77E-01	4.65E-03	6.35E-01	7.91E-03	15	18	15	17
translation initiation factor activity	MF	6.53E-02	7.67E-04	1.29E-01	1.31E-03	15	18	15	17
translation factor activity, RNA binding	MF	1.56E-02	4.27E-04	3.82E-02	1.81E-03	21	24	21	22
eukaryotic translation initiation factor 3 complex	CC	3.41E-02	2.91E-04	5.50E-01	1.71E-04	8	10	7	10
2.dicarboxylic acid metabolic process	BP	2.90E-02	9.31E-03	1.31E-02	3.11E-03	15	16	16	16
3. actin nucleation	BP	1.14E-02	1.23E-03	2.23E-02	8.31E-03	10	11	10	10
Offshore Corals (O→N, O→O)									
1. purine nucleoside monophosphate biosynthetic process	BP	6.19E-01	1.00E+00	5.60E-03	5.19E-03	16	16	20	19
purine ribonucleoside monophosphate biosynthetic process	BP	6.19E-01	1.00E+00	5.60E-03	5.19E-03	16	16	20	19
2. intracellular protein transport	BP	1.87E-01	8.90E-02	4.89E-03	7.65E-03	54	57	62	57
Nearshore Site (N→N, O→N)									
1. translational initiation	BP	2.77E-01	4.65E-03	6.35E-01	7.91E-03	15	18	15	17
translation initiation factor activity	MF	6.53E-02	7.67E-04	1.29E-01	1.31E-03	15	18	15	17
Nearshore Corals (N→N, N→O)									
1. oxidoreduction coenzyme metabolic process	BP	7.55E-04	7.96E-03	1.20E-02	4.09E-02	22	21	21	19
NAD binding	MF	9.43E-03	6.96E-04	8.86E-02	2.29E-02	18	20	17	17
2. lyase activity	MF	3.01E-03	5.56E-04	6.59E-01	1.34E-02	45	48	40	42
Nearshore vs Offshore Corals (N→N, O→O)									
1. clathrin coat	CC	7.04E-03	1.10E-02	1.53E-02	6.98E-03	9	9	9	9
2. catalytic step 2 spliceosome	CC	8.96E-03	9.04E-02	6.13E-01	8.80E-03	12	11	10	12
Cross-transplanted corals (O→N, N→O)									
1. monocarboxylic acid catabolic process	BP	1.42E-01	**7.32E-03**	1.62E-02	**1.71E-04**	13	15	14	17
fatty acid beta-oxidation	BP	1.72E-01	**5.17E-03**	1.66E-02	**7.10E-04**	11	13	12	14
fatty-acyl-CoA binding	MF	1.40E-01	**6.58E-03**	1.44E-02	**1.09E-03**	12	14	13	15
2. cellular amino acid biosynthetic process	BP	1.00E+00	**3.35E-04**	2.57E-02	**7.20E-03**	23	32	27	30
3. tricarboxylic acid cycle	BP	7.39E-02	**4.07E-03**	2.59E-01	**5.72E-03**	14	16	13	16

4. oxidoreductase activity, acting on the CH-CH group of donors, with a flavin as acceptor	MF	2.99E-01	**9.89E-03**	2.92E-02	**1.29E-03**	10	12	11	13
Unique in N→N									
1. pyridine nucleotide metabolic process	BP	1.04E-03	1.12E-02	1.64E-02	7.22E-02	20	19	19	17
nicotinamide nucleotide metabolic process	BP	1.04E-03	1.12E-02	1.64E-02	7.22E-02	20	19	19	17
2. peptidase inhibitor activity	MF	7.67E-03	1.57E-02	2.13E-02	1.57E-02	25	25	25	25
3. transferase activity, transferring nitrogenous groups	MF	9.91E-03	1.53E-02	1.83E-02	1.53E-02	12	12	12	12
Unique in N→O									
1. organic acid biosynthetic process	BP	1.00E+00	**1.26E-03**	7.67E-02	4.96E-02	29	39	33	36
carboxylic acid biosynthetic process	BP	1.00E+00	**1.26E-03**	7.67E-02	4.96E-02	29	39	33	36
alpha-amino acid biosynthetic process	BP	8.37E-02	**2.16E-03**	1.41E-01	3.90E-02	21	30	25	28
2. regulation of cytoskeleton organization	BP	2.09E-02	**3.30E-03**	4.52E-02	7.44E-02	22	24	21	22
positive regulation of cytoskeleton organization	BP	2.45E-02	**7.32E-03**	9.77E-02	6.20E-02	14	15	13	14
3. translational initiation	BP	3.62E-01	**7.17E-03**	1.07E-02	8.85E-01	15	18	17	15
eukaryotic 43S preinitiation complex	CC	3.58E-02	**3.35E-03**	3.44E-02	6.90E-02	7	8	7	7
4. NAD binding	MF	1.28E-02	**1.12E-03**	2.94E-02	1.27E-01	18	20	17	17
5. actin nucleation	BP	1.42E-02	**1.69E-03**	1.03E-02	2.96E-02	10	11	10	10
6. chitinase activity	MF	5.26E-02	**5.13E-03**	4.14E-01	8.62E-02	8	9	7	8
7. carbohydrate derivative catabolic process	BP	8.37E-02	**7.17E-03**	2.42E-01	1.03E-02	16	18	15	18
8. endocytosis	BP	1.45E-01	**7.83E-03**	1.94E-01	1.00E+00	31	35	30	30
9. pyridoxal phosphate binding	MF	1.50E-01	**8.56E-04**	2.14E-01	1.47E-02	23	28	22	26
Unique in O→O									
1. guanyl nucleotide binding	MF	1.11E-01	1.00E+00	**1.59E-03**	1.00E+00	74	71	78	72
guanyl ribonucleotide binding	MF	1.11E-01	1.00E+00	**1.59E-03**	1.00E+00	74	71	78	72
GTP binding	MF	1.39E-01	1.00E+00	**2.09E-03**	1.00E+00	73	70	77	71
2. vesicle organization	BP	2.42E-01	3.50E-02	**8.89E-03**	6.72E-01	18	20	20	18
cytoplasmic vesicle	CC	7.27E-02	4.70E-02	**2.48E-04**	7.42E-02	18	19	22	19
cytoplasmic membrane-bounded vesicle	CC	5.50E-02	3.49E-02	**1.66E-04**	5.53E-02	18	19	22	19
Unique in O→N									
1.lipid oxidation	BP	7.01E-01	3.29E-02	6.19E-03	8.98E-02	11	13	14	12
fatty acid catabolic process	BP	4.26E-01	1.69E-02	2.87E-03	4.99E-02	11	13	14	12
fatty acid oxidation	BP	7.01E-01	3.29E-02	6.19E-03	8.98E-02	11	13	14	12
fatty acid beta-oxidation using acyl-CoA dehydrogenase	BP	4.89E-01	1.45E-02	2.04E-03	5.23E-02	10	12	13	11
2. macromolecular complex subunit organization	BP	2.89E-02	2.43E-02	4.57E-03	2.12E-02	98	102	107	96
macromolecular complex assembly	BP	9.21E-02	2.15E-01	1.23E-03	6.03E-02	66	67	76	65
cellular macromolecular complex assembly	BP	1.13E-02	9.26E-02	3.56E-03	4.98E-02	51	50	55	48
protein complex subunit organization	BP	1.00E+00	7.06E-01	7.24E-03	9.73E-01	54	58	66	54
3. response to toxic substance	BP	2.46E-01	1.00E+00	7.83E-03	1.00E+00	23	20	27	20
detoxification	BP	1.43E-01	1.00E+00	3.83E-03	1.00E+00	23	20	27	20

cellular oxidant detoxification	BP	1.43E-01	1.00E+00	3.83E-03	1.00E+00	23	20	27	20
cellular detoxification	BP	1.43E-01	1.00E+00	3.83E-03	1.00E+00	23	20	27	20
4. purine-containing compound metabolic process	BP	1.76E-02	5.97E-02	2.19E-04	9.45E-02	45	45	52	42
purine nucleoside biosynthetic process	BP	5.09E-02	1.02E-01	1.00E-04	3.06E-02	20	20	25	20
purine ribonucleoside biosynthetic process	BP	5.09E-02	1.02E-01	1.00E-04	3.06E-02	20	20	25	20
5. catalytic activity	MF	1.63E-02	1.02E-02	1.69E-03	5.83E-01	909	945	968	854
intramolecular transferase activity, phosphotransferases	MF	1.01E-01	1.30E-01	4.05E-03	7.81E-02	6	6	7	6
oxidoreductase complex	CC	2.89E-01	1.56E-02	3.51E-03	2.87E-01	10	12	13	10
6. antioxidant activity	MF	8.24E-02	1.00E+00	1.76E-03	1.00E+00	23	20	27	20
7. extracellular organelle	CC	4.56E-02	8.94E-02	2.49E-03	5.19E-01	17		20	15
extracellular vesicle	CC	4.56E-02	8.94E-02	2.49E-03	5.19E-01	17	17	20	15
extracellular membrane-bounded organelle	CC	3.36E-02	6.64E-02	7.25E-03	1.00E+00	17	17	19	14
extracellular exosome	CC	3.36E-02	6.64E-02	7.25E-03	1.00E+00	17	17	19	14
8. mitochondrion	CC	1.12E-01	2.75E-02	4.13E-04	5.33E-01	62	67	75	59
9. membrane protein complex	CC	4.77E-01	1.01E-02	2.91E-03	2.60E-01	67	77	81	68
10. transport vesicle membrane	CC	1.00E+00	1.00E+00	4.95E-03	1.11E-01	3	3	6	5

Figure S1. Venn diagram of coral proteins identified from the mass spectrometry based shotgun proteomics in coral samples.

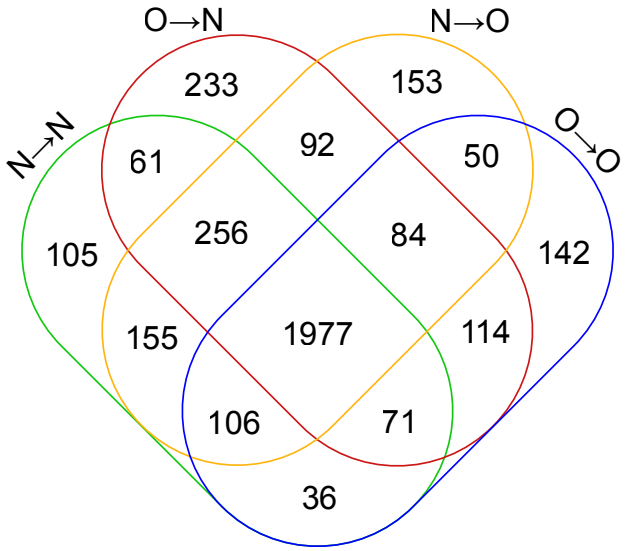

Figure S2. NMDS Plot of protein abundances of the 12 coral samples used in LC-MS/MS. Nearshore corals (green) and offshore corals (blue) showed a significant separation (R = 0. 7074 P = 0.004), regardless of the transplant sites.

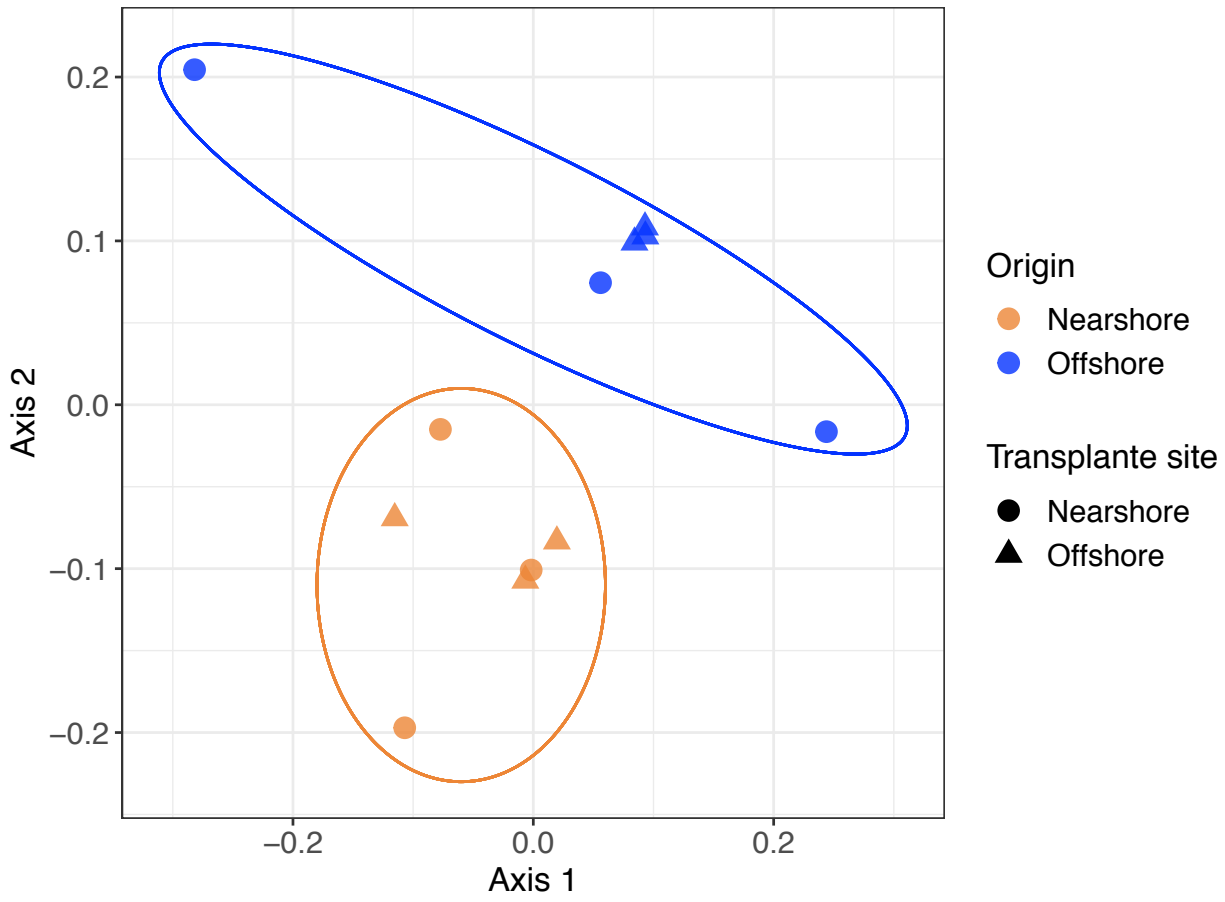

Figure S3. Diagram of enriched GO terms in the Biological Process category identified with significantly more abundant proteins in the offshore corals at the nearshore site (O→N), compared to the nearshore corals (N→N).

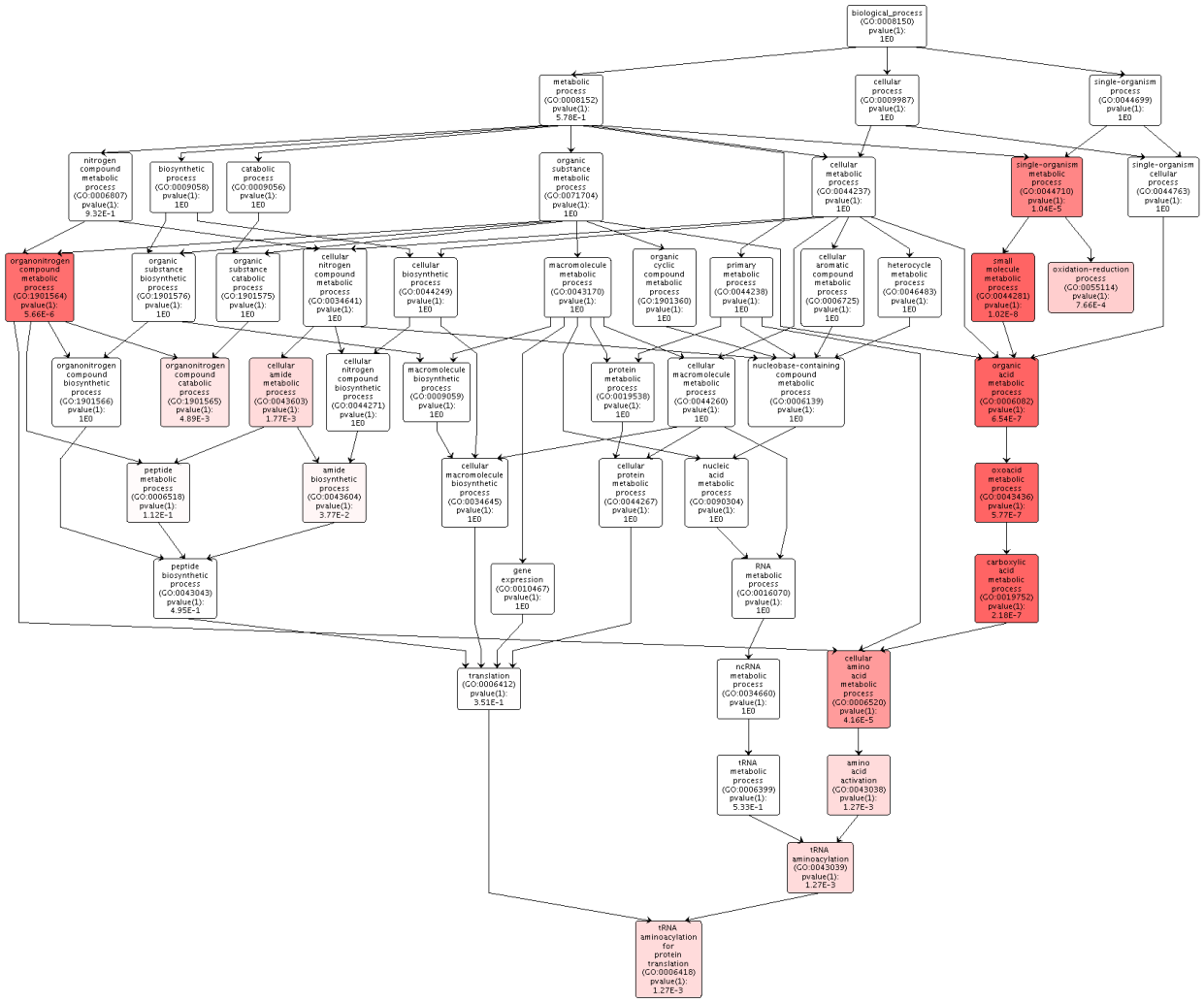

Figure S4. Metabolic pathway map generated by iPath3 with significantly differentially expressed proteins of corals at the nearshore site (A). Blue lines indicate the pathways identified from significantly more abundant proteins in the offshore corals, and orange lines indicate those in the nearshore corals. A metabolic pathway map was also generated using all identified proteins at the nearshore site (B). Blue lines indicate the uniquely identified pathways in the offshore corals, orange lines indicate those in the nearshore corals, and gray lines indicate the pathways identified in both corals.

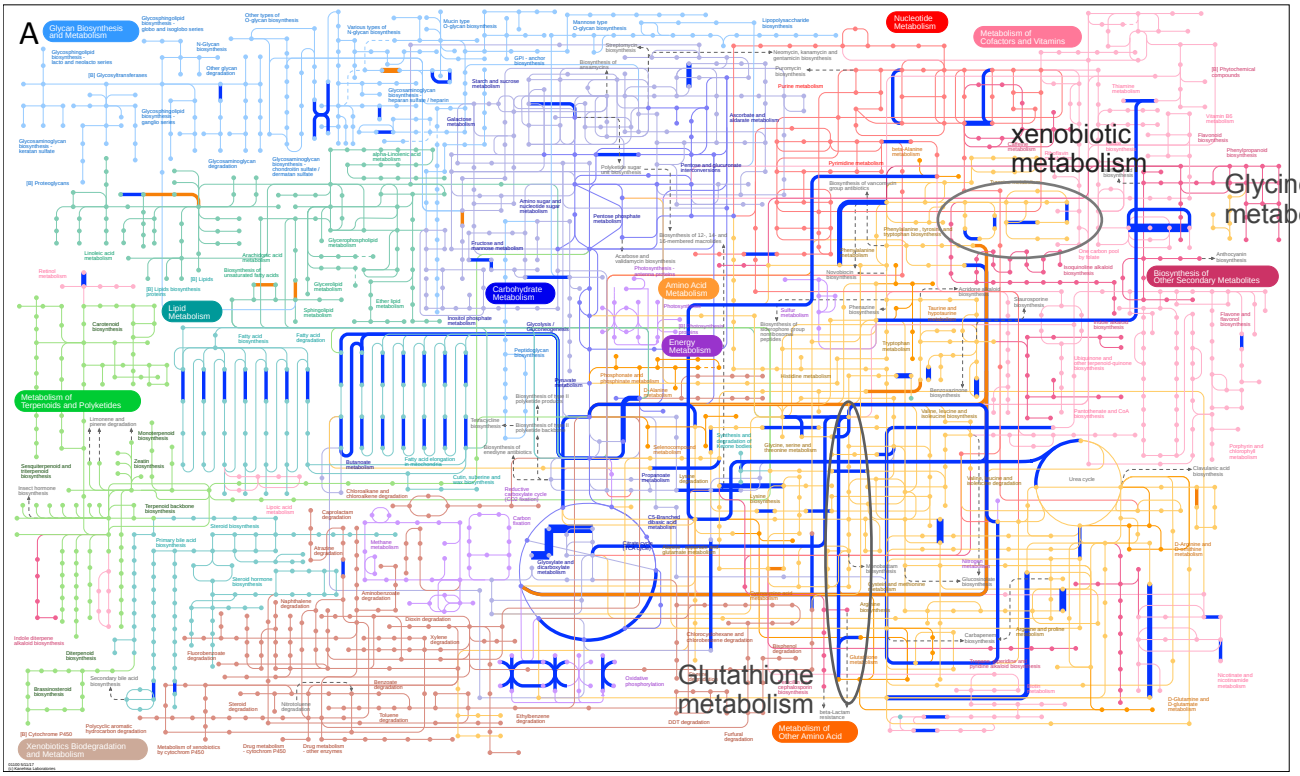

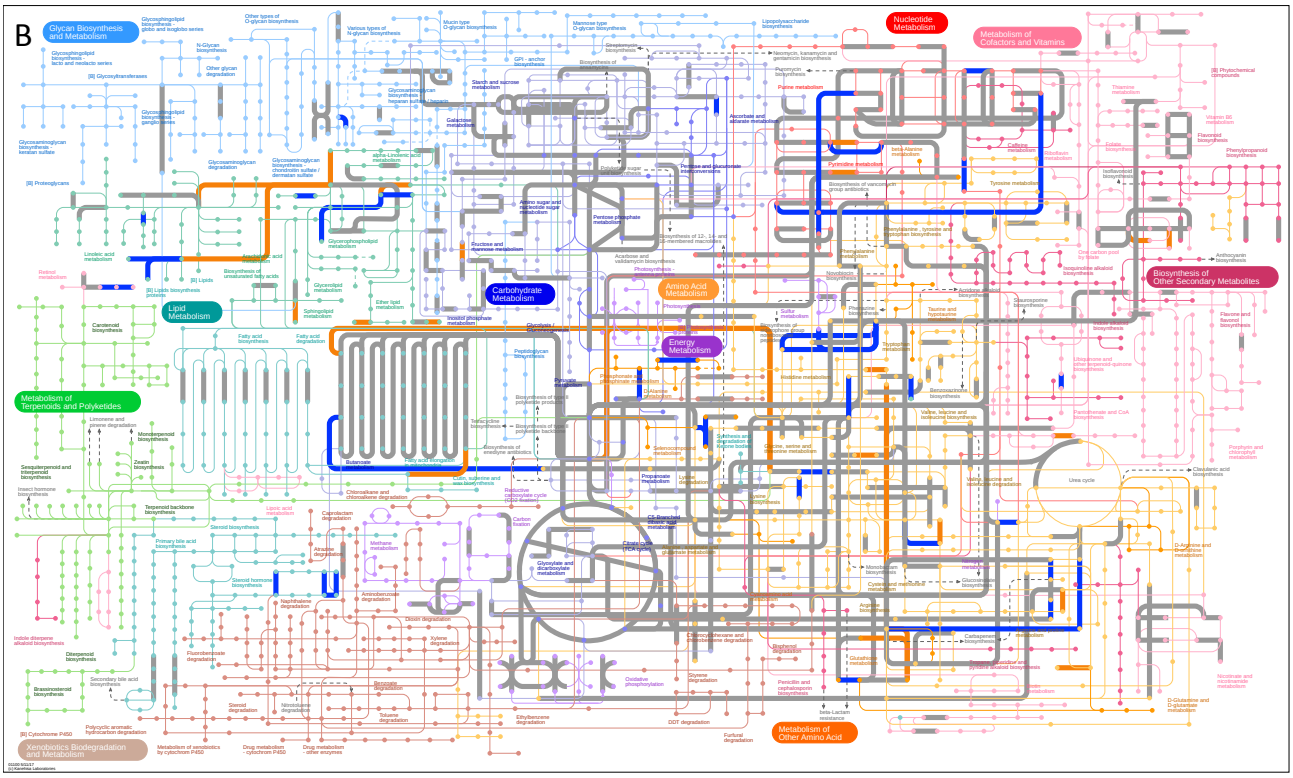

Figure S5. Diagram of enriched GO terms in the Biological Process category, identified with significantly more abundant proteins in the offshore corals at the offshore sit e (O→O), compared to the nearshore corals (N→O).

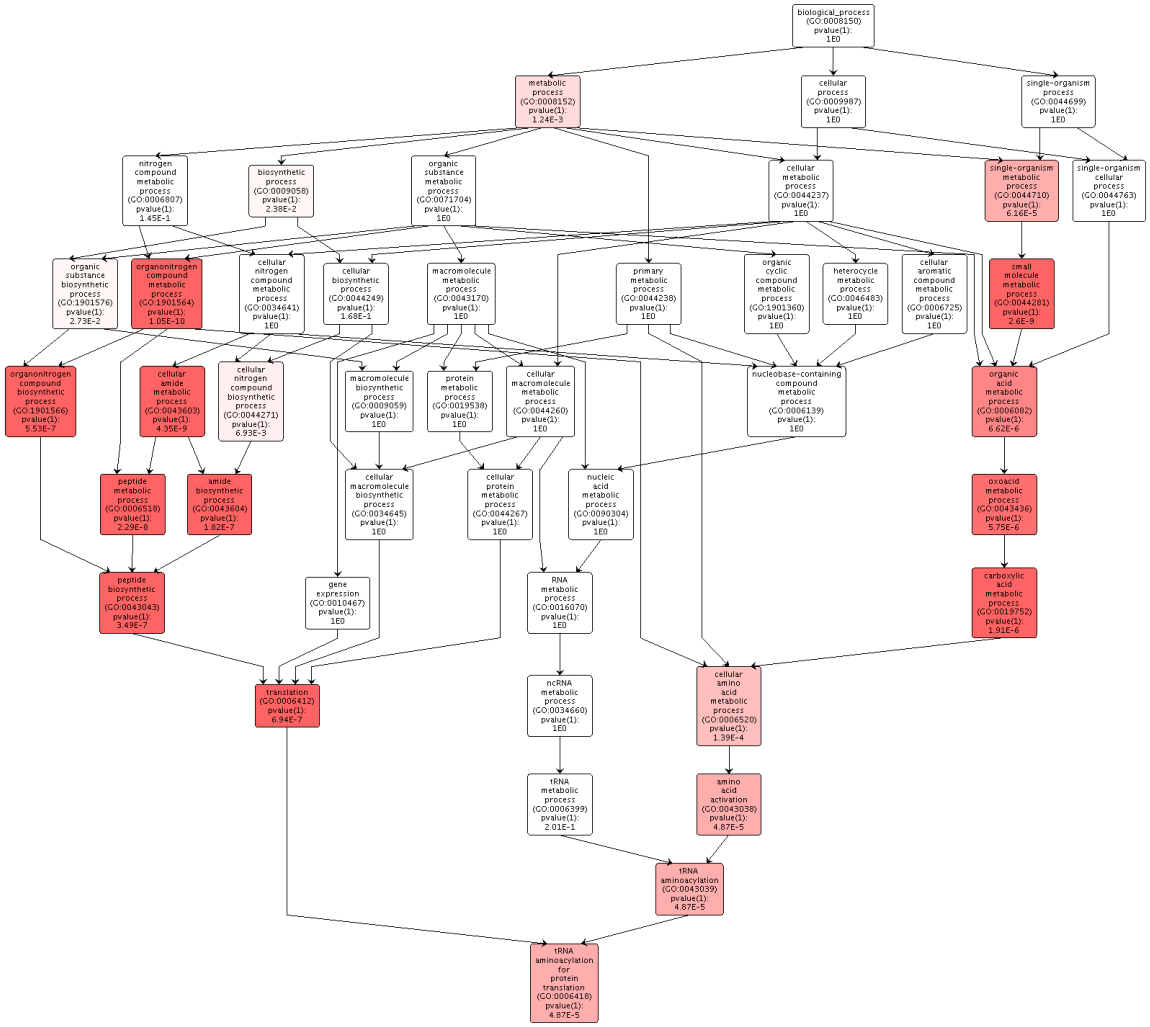

Figure S6. Metabolic pathway map generated by iPath3 with significantly differentially expressed proteins of corals at the offshore site (A). Blue lines indicate the pathways identified from significantly more abundant proteins in the offshore corals, and orange lines indicate those in the nearshore corals. A metabolic pathway map was also generated using all identified proteins at the offshore site (B). Blue lines indicate the uniquely identified pathways in the offshore corals, orange lines indicate those in the nearshore corals, and gray lines indicate the pathways identified in both corals.

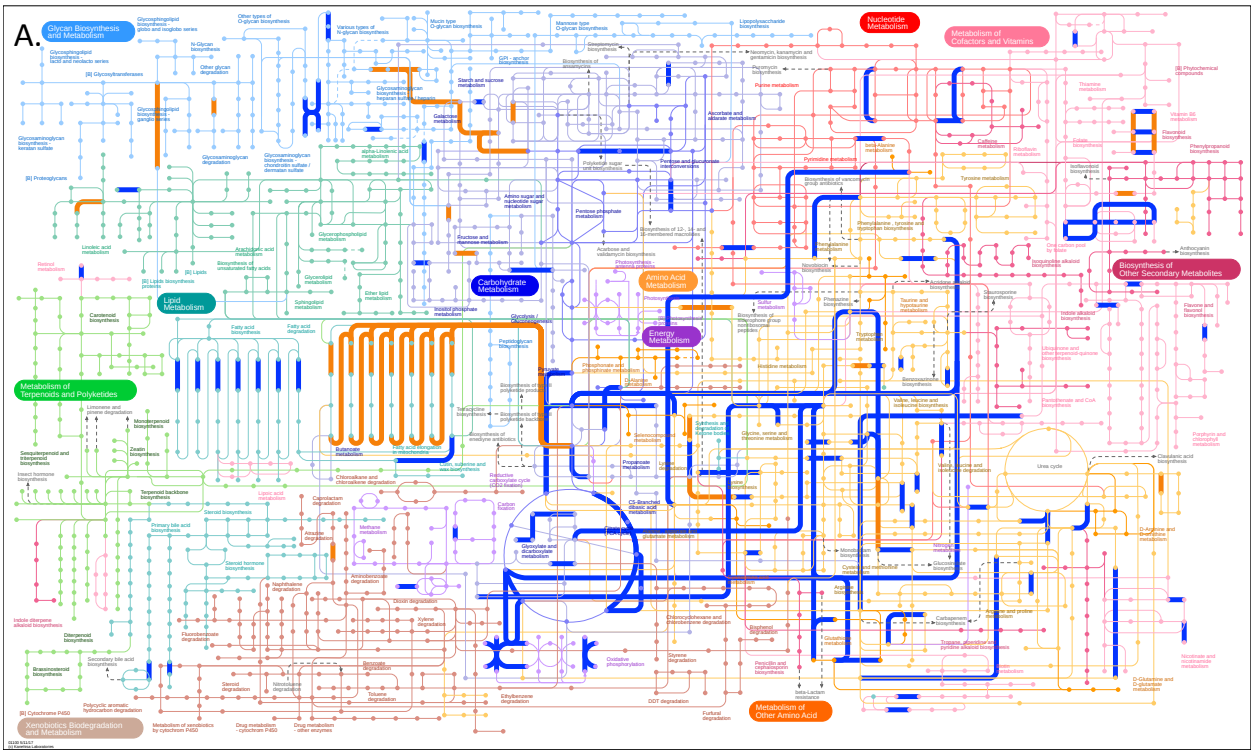

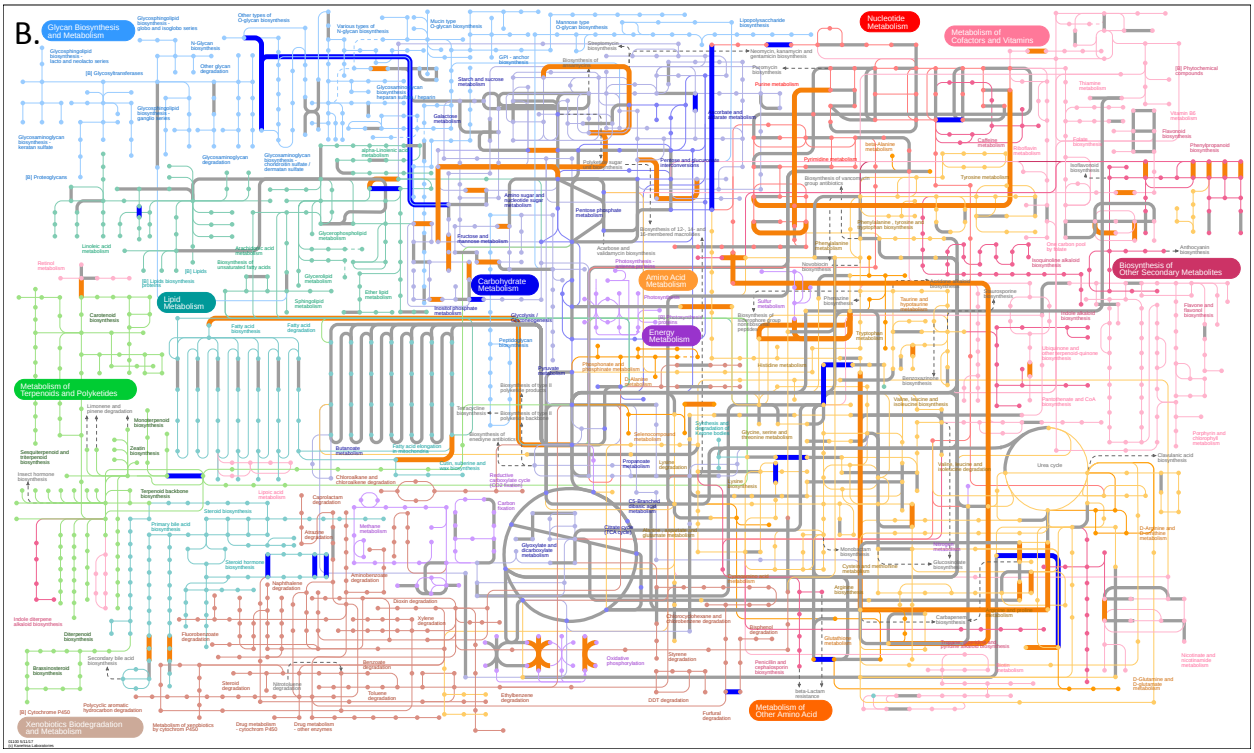

Figure S7. Fold changes in protein abundance between the nearshore and offshore coral populations

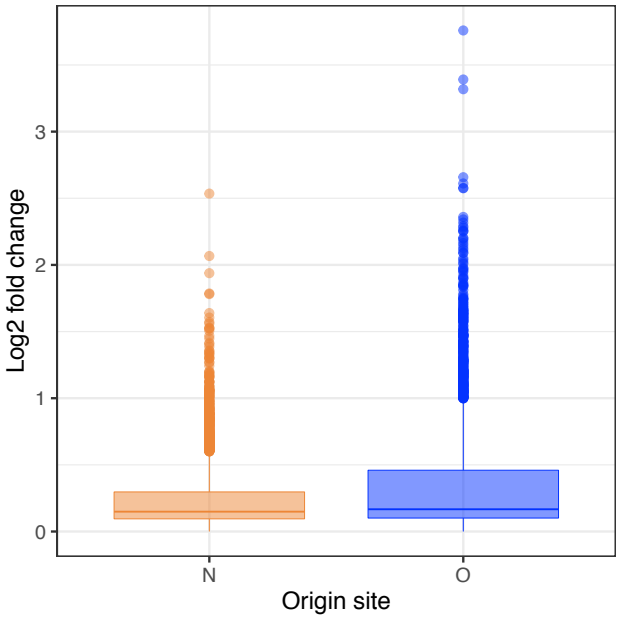

Figure S8. Alignment of the proteins with the same annotation. A) peroxiredoxin-1, and B) peroxiredoxin-4.

A.

```
m.6174      1 MAAASIALITRRIAPQ-ICRNPLNLQR---LRTAFPLCTASRKAFSSDPI-MSKAFIQKP
m.17739     1 MACGVVFFVVLAFVPAGIFANKVEDDEETCRRYANGQVYPEKTTISEHAVHWSKAQISKP

m.6174     56 APAFAGTAVNHHGEFIDVKLSDYKGKYLVLFFYPLDFTFVCPTEIIAFSDRVEEFRAINC
m.17739    61 APHWEGTAVV-KGEFKELKLSDFKGKYLVFFFYPLDFTFVCPTEIIAFSDRIEEFRAINT

m.6174    116 EVIACSVDSHFSHLAWTEKPRKKGGLGTMNIPLLSDITKQISKDYGVLLEDQGVALRGLF
m.17739   120 EVVGCSVDSVFTHLAWINTPRKEGGLGRLQYPLLSDLNHQIAKDYGVLLENEGHTLRGLF

m.6174    176 IIDDKGILRQITMNDLPVGRSVDEVLRLVQAFQFTDKHGEVCPAGWRPGNDTIVPDAKKS
m.17739   180 IIDDKGTLRQITMNDLPVGRSVDETLRLVQAFQYTDKHGEVCPAGWKPGKETIIPDPTEK

m.6174    236 ADYFSKQSXXXXXXXX
m.17739   240 KKYFAKQAEKGEKEKE
```

B.

```
m.17686     1 VMKHPHGCQFKNLLPAQVDGFC-PTRNFFEPCFFSGDIRN-NENPGLNSIHTIFVREHNR
m.9432      1 VMKHPDGKPFRNLLPPQTEESGCPSLDPQRPCFLSGD-ERNNENPGLNSVHTIFVRQHNR

m.17686    59 IATFFIKNTDWDPEKVFQ---ETRRIVGAQLQIITYGEFLPLLLSEHTRKERGLVLLEGE
m.9432     60 IATFLLNNNNANRWEKDRIFNETRKIIGAQLQVITYNEFLPLILSRKTIKKFGLELLKGT

m.17686   116 EFFTGYDKEVNAQILTAFAVAGYRFGHSLVQ-------ELFNRFSQDGFEHKCSKCSKDK
m.9432    120 QFFNGYDKNVNAQMTNAFSVAAYRFGH--------SLVQEWFKRFSQIGFEHKRTECGLK

m.17686   169 LQFQPIPVLDFNNPAPLFDVCKGGVDAILRGLL-------KDPAAKADGRFSSSVQENLS
m.9432    172 TEFRPIPVLDFNNPQYLYETDQGGVDAIVRGLV-------KDSAAKSDGRFSSSVQENLR

m.17686   222 RGEGDTSDLIAINLRRGH-DRGLPSYTSFRRFCGLPLVRRFSDLVTVAHFDEKVVARLQE
m.9432    225 RGEGDLSDLVSINIQRGR-ERGLPGYTKYRNLQLCGLSNVKSFEDLKNVAGFQQEDVENL

m.17686   281 VYK--RVGDIDLFSGGMLEPSDPKGGELSATFQCILANQFKRTKFGDRFWHENAPNVTLN
m.9432    284 RKVYDNVHDIDLFVGGMLEPRPSDGGVLGPTFQCIVAEQFRRLRVGDRFWHENAPNENLN

m.17686   339 TDKTAFNSCQLKEIRKTRFSRIICDNSDDITSIQKDALMQSSVRVSCDELPKINLKAW--
m.9432    344 TDQTAYNEAMLQEIRKTTFARILCDNADSITAVNKMVFQQSKERVNCDQ--LPRVSLNPW

m.17686   397 ITDCPSSDSVYSDEPQDTHDEFXXX
m.9432    402 IERHRDSGEPDDVDDDLLDDEDPEF
```

Figure S9. Temperatures and light intensity during the reciprocal transplant experiment of the nearshore and offshore sites of Maunalua Bay.

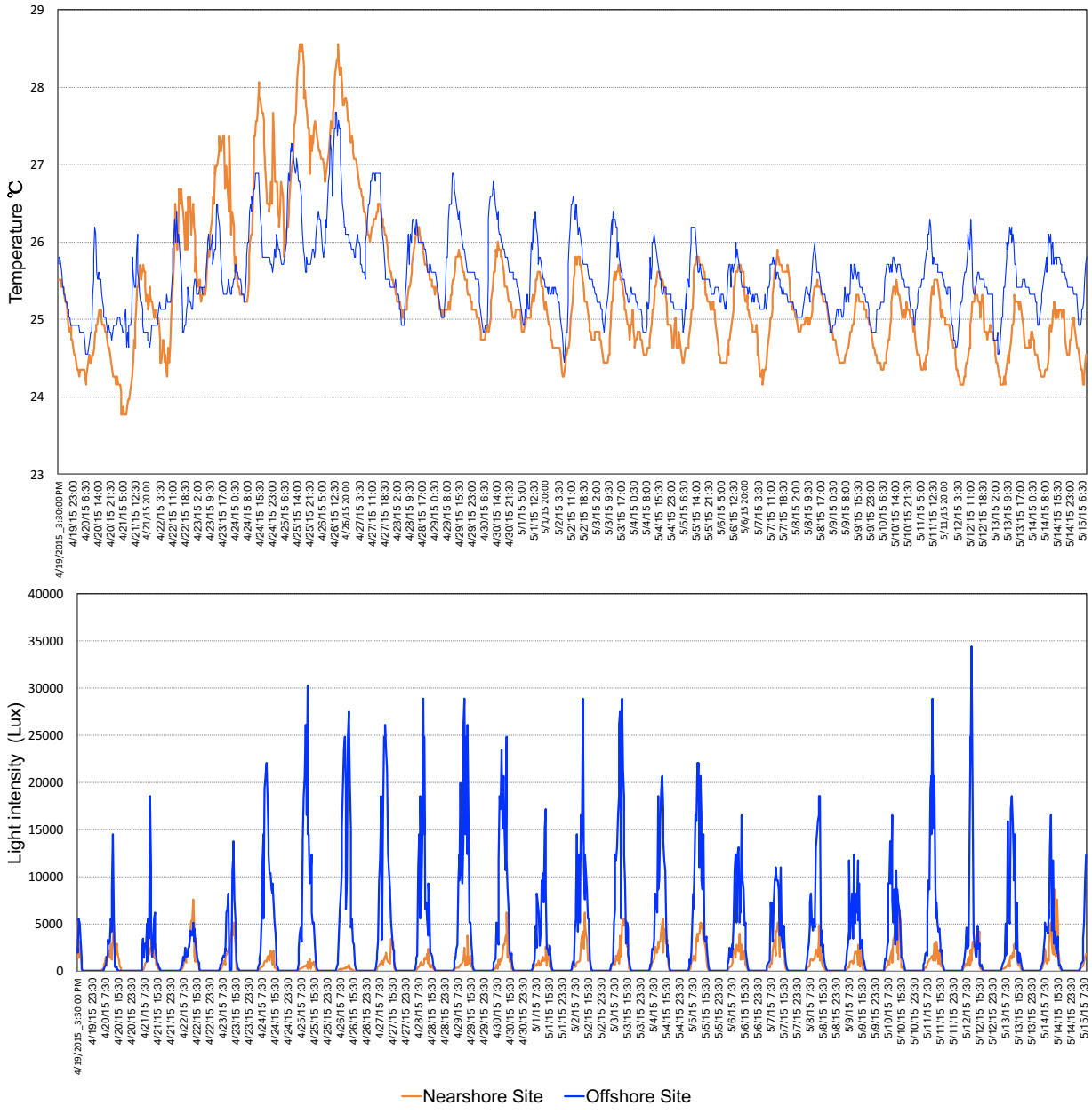

Figure S10. Tissue lipid content of *P. lobata* before and after the reciprocal transplant experiment in Maunalua Bay. Different letters indicate statistical significant difference. N = nearshore, O=offshore. Arrows point the transplant direction; e.g. N→N indicates Nearshore corals transplanted to the nearshore site.

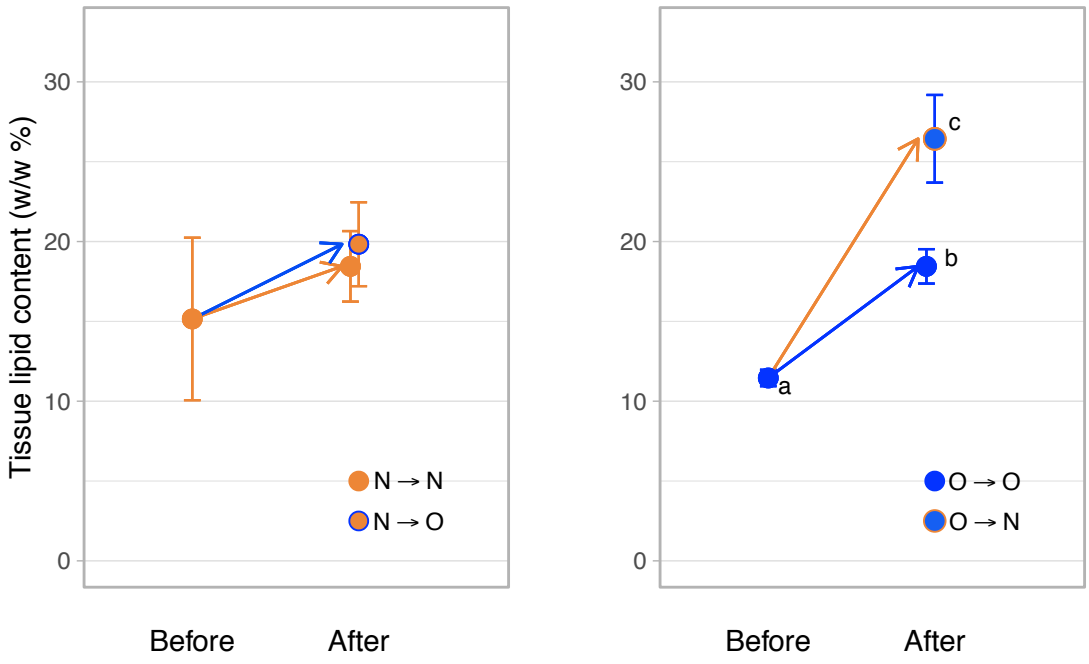

Fig. S11 Diagrams of overlapping proteins identified between the pair of treatments

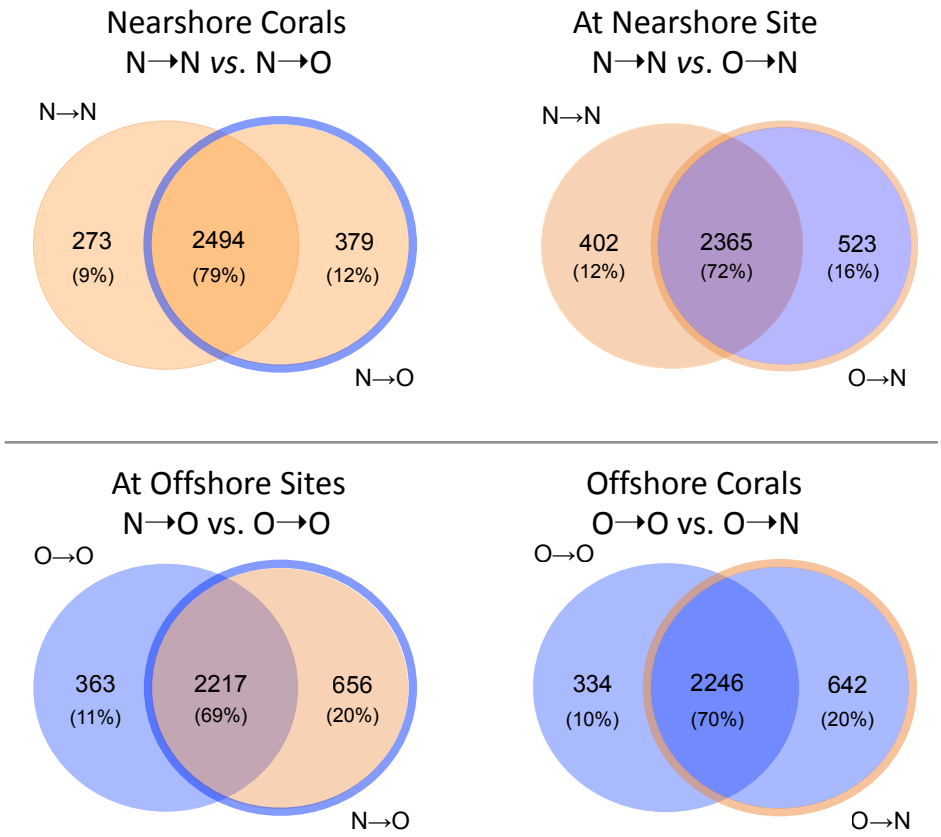

Table S1. ANOVA results of tissue layer thickness and total lipid content of *P. lobata*, comparing between the nearshore and offshore populations, and between the nearshore and offshore transplant sites in Maunalua Bay. A) Results of the tissue layer thickness comparison, nested 2-way ANOVA, followed by Tukey HSD. B) Results of the total lipid content comparison, 2-way ANOVA , followed by Tukey HSD).

A.

ANOVA	Df	Mean Sq	F value	Pr(>F)
Population	1	3.336	44.90	**2.57e-10*** **
Transplant Site	1	2.132	28.70	**2.56e-07*** **
Interaction (Population:Site)	1	1.399	1.399	**2.37e-05*** **
Interaction (Population:Site:Indiv)	16	4.494	60.49	**< 2e-16*** **
Residuals	180	0.074		

Turkey HSD Comparison	Diff.	P adj
NN - NO	0.4256	**0.0000000**
NN - ON	-0.0392	0.8893995
NN - OO	0.0518	0.7777140
NO - OO	-0.3738	**0.0000000**
ON - OO	0.0910	0.3429679
NO - ON	0.4648	**0.0000000**

B.

	Df	Mean Sq	F value	Pr(>F)
Population	1	0.01543	2.179	0.1594
Transplant-site	1	0.01706	2.409	0.1402
Interaction	1	0.03305	4.668	**0.0462***

Turkey HSD Comparison	Diff.	P adj
NN - NO	0.13685	0.0861
NN - ON	0.02289	0.9724
NN - OO	-0.00286	0.9999
NO - OO	-0.13972	0.0779
ON - OO	-0.02576	0.9615
NO - ON	-0.11396	0.1824

Table S2. The enriched GO terms uniquely identified in the offshore corals (O→N) and the nearshore corals (N→N) at the nearshore site.

Treat-ment	GO Accession	GO Name	GO Ca.	P-value	N. of proteins
ON	GO:0046129	purine ribonucleoside biosynthetic process	BP	1.00E-04	25
ON	GO:0042451	purine nucleoside biosynthetic process	BP	1.00E-04	25
ON	GO:0072329	monocarboxylic acid catabolic process	BP	1.11E-04	17
ON	GO:0046395	carboxylic acid catabolic process	BP	1.87E-04	28
ON	GO:0016054	organic acid catabolic process	BP	1.87E-04	28
ON	GO:0072521	purine-containing compound metabolic process	BP	2.19E-04	52
ON	GO:0006635	fatty acid beta-oxidation	BP	4.89E-04	14
ON	GO:0044283	small molecule biosynthetic process	BP	9.98E-04	47
ON	GO:0065003	macromolecular complex assembly	BP	1.23E-03	76
ON	GO:0033539	fatty acid beta-oxidation using acyl-CoA dehydrogenase	BP	2.04E-03	13
ON	GO:0009062	fatty acid catabolic process	BP	2.87E-03	14
ON	GO:0034622	cellular macromolecular complex assembly	BP	3.56E-03	55
ON	GO:1990748	cellular detoxification	BP	3.83E-03	27
ON	GO:0098869	cellular oxidant detoxification	BP	3.83E-03	27
ON	GO:0098754	detoxification	BP	3.83E-03	27
ON	GO:0006099	tricarboxylic acid cycle	BP	3.86E-03	16
ON	GO:0043933	macromolecular complex subunit organization	BP	4.57E-03	107
ON	GO:0006886	intracellular protein transport	BP	4.89E-03	62
ON	GO:0009127	purine nucleoside monophosphate biosynthetic process	BP	5.60E-03	20
ON	GO:0009168	purine ribonucleoside monophosphate biosynthetic process	BP	5.60E-03	20
ON	GO:0019395	fatty acid oxidation	BP	6.19E-03	14
ON	GO:0034440	lipid oxidation	BP	6.19E-03	14
ON	GO:1901136	carbohydrate derivative catabolic process	BP	6.79E-03	18
ON	GO:0071822	protein complex subunit organization	BP	7.24E-03	66
ON	GO:0009636	response to toxic substance	BP	7.83E-03	27
ON	GO:1901605	alpha-amino acid metabolic process	BP	8.76E-03	44
ON	GO:0016614	oxidoreductase activity, acting on CH-OH group of donors	MF	2.12E-06	35
ON	GO:0000062	fatty-acyl-CoA binding	MF	7.53E-04	15
ON	GO:0052890	oxidoreductase activity, acting on the CH-CH group of donors, with a flavin as acceptor	MF	9.26E-04	13
ON	GO:0050662	coenzyme binding	MF	1.50E-03	57
ON	GO:0003824	catalytic activity	MF	1.69E-03	968

ON	GO:0016209	antioxidant activity	MF	1.76E-03	27
ON	GO:0016868	intramolecular transferase activity, phosphotransferases	MF	4.05E-03	7
ON	GO:0030170	pyridoxal phosphate binding	MF	8.86E-03	26
ON	GO:0005739	mitochondrion	CC	4.13E-04	75
ON	GO:0043230	extracellular organelle	CC	2.49E-03	20
ON	GO:1903561	extracellular vesicle	CC	2.49E-03	20
ON	GO:0098796	membrane protein complex	CC	2.91E-03	81
ON	GO:1990204	oxidoreductase complex	CC	3.51E-03	13
ON	GO:0030658	transport vesicle membrane	CC	4.95E-03	6
ON	GO:0070062	extracellular exosome	CC	7.25E-03	19
ON	GO:0065010	extracellular membrane-bounded organelle	CC	7.25E-03	19
NN	GO:0071826	ribonucleoprotein complex subunit organization	BP	6.94E-05	31
NN	GO:0006733	oxidoreduction coenzyme metabolic process	BP	7.55E-04	22
NN	GO:0019362	pyridine nucleotide metabolic process	BP	1.04E-03	20
NN	GO:0046496	nicotinamide nucleotide metabolic process	BP	1.04E-03	20
NN	GO:0032271	regulation of protein polymerization	BP	4.93E-03	16
NN	GO:0034314	Arp2/3 complex-mediated actin nucleation	BP	6.58E-03	8
NN	GO:0016836	hydro-lyase activity	BP	1.04E-04	17
NN	GO:0004867	serine-type endopeptidase inhibitor activity	MF	1.27E-03	11
NN	GO:0016835	carbon-oxygen lyase activity	MF	1.31E-03	18
NN	GO:0016829	lyase activity	MF	3.01E-03	45
NN	GO:0030414	peptidase inhibitor activity	MF	7.67E-03	25
NN	GO:0051287	NAD binding	MF	9.43E-03	18
NN	GO:0016769	transferase activity, transferring nitrogenous groups	MF	9.91E-03	12
NN	GO:0008540	proteasome regulatory particle, base subcomplex	CC	5.62E-03	8
NN	GO:0070993	translation preinitiation complex	CC	5.62E-03	8
NN	GO:0033290	eukaryotic 48S preinitiation complex	CC	5.62E-03	8
NN	GO:0005768	endosome	CC	6.73E-03	23
NN	GO:0030118	clathrin coat	CC	7.04E-03	9
NN	GO:0071013	catalytic step 2 spliceosome	CC	8.96E-03	12

Table S3 The Gene Ontology (GO) terms identified with significantly more abundant proteins in the offshore population at the nearshores site (O→N), compared to the nearshore population (N→N) using metaGOmics (cutoff P < 0.01). BP=Biological process, MF= Molecular Function, and CC = Cellular Component of the GO categories.

GO Accession	GO Terms	GO Ca.	P-value	No. of Protein	%
GO:0044281	small molecule metabolic process	BP	1.02E-08	41	14.9%
GO:0019752	carboxylic acid metabolic process	BP	2.18E-07	27	9.8%
GO:0043436	oxoacid metabolic process	BP	5.77E-07	27	9.8%
GO:0006082	organic acid metabolic process	BP	6.54E-07	27	9.8%
GO:1901564	organonitrogen compound metabolic process	BP	5.66E-06	41	14.9%
GO:0044710	single-organism metabolic process	BP	1.04E-05	72	26.1%
GO:0006520	cellular amino acid metabolic process	BP	4.16E-05	18	6.5%
GO:0055114	oxidation-reduction process	BP	7.66E-04	37	13.4%
GO:0043038	amino acid activation	BP	1.27E-03	8	2.9%
GO:0043039	tRNA aminoacylation	BP	1.27E-03	8	2.9%
GO:0006418	tRNA aminoacylation for protein translation	BP	1.27E-03	8	2.9%
GO:0043603	cellular amide metabolic process	BP	1.77E-03	22	8.0%
GO:1901565	organonitrogen compound catabolic process	BP	4.89E-03	10	3.6%
GO:0016874	ligase activity	MF	3.29E-04	18	6.5%
GO:0016491	oxidoreductase activity	MF	3.56E-04	36	13.0%
GO:0016875	ligase activity, forming carbon-oxygen bonds	MF	6.29E-04	8	2.9%
GO:0016876	ligase activity, forming aminoacyl-tRNA and related compounds	MF	6.29E-04	8	2.9%
GO:0004812	aminoacyl-tRNA ligase activity	MF	6.29E-04	8	2.9%
GO:0005737	cytoplasm	CC	2.75E-10	69	25.0%
GO:0048475	coated membrane	CC	2.95E-05	8	2.9%
GO:0030117	membrane coat	CC	2.95E-05	8	2.9%
GO:0005622	intracellular	CC	6.85E-05	93	33.7%
GO:0030118	clathrin coat	CC	4.24E-04	5	1.8%
GO:0030120	vesicle coat	CC	4.24E-04	5	1.8%
GO:0030662	coated vesicle membrane	CC	6.27E-04	5	1.8%
GO:0044424	intracellular part	CC	6.43E-04	82	29.7%
GO:0030659	cytoplasmic vesicle membrane	CC	1.26E-03	5	1.8%

GO:0012506	vesicle membrane	CC	1.26E-03	5	1.8%
GO:0005623	cell	CC	1.56E-03	98	35.5%
GO:0030135	coated vesicle	CC	1.72E-03	5	1.8%
GO:0030660	Golgi-associated vesicle membrane	CC	1.77E-03	4	1.4%
GO:0005798	Golgi-associated vesicle	CC	2.91E-03	4	1.4%
GO:0044433	cytoplasmic vesicle part	CC	3.03E-03	5	1.8%
GO:0044464	cell part	CC	4.45E-03	96	34.8%
GO:0044444	cytoplasmic part	CC	6.07E-03	41	14.9%

Table S4. The enriched GO terms uniquely identified in the offshore corals (O→O) and the nearshore corals (N→O) at the offshore site.

Treat-ment	GO Accession	GO Name	GO Ca.	P-value	N. of proteins
NO	GO:0019318	hexose metabolic process	BP	1.19E-04	23
NO	GO:0009141	nucleoside triphosphate metabolic process	BP	1.37E-04	33
NO	GO:0006101	citrate metabolic process	BP	2.05E-04	18
NO	GO:0005996	monosaccharide metabolic process	BP	3.67E-04	26
NO	GO:0009205	purine ribonucleoside triphosphate metabolic process	BP	3.84E-04	30
NO	GO:0008652	cellular amino acid biosynthetic process	BP	6.45E-04	31
NO	GO:0009144	purine nucleoside triphosphate metabolic process	BP	8.11E-04	30
NO	GO:0046394	carboxylic acid biosynthetic process	BP	1.82E-03	38
NO	GO:0016053	organic acid biosynthetic process	BP	1.82E-03	38
NO	GO:0051493	regulation of cytoskeleton organization	BP	1.94E-03	24
NO	GO:0006099	tricarboxylic acid cycle	BP	2.72E-03	16
NO	GO:0006635	fatty acid beta-oxidation	BP	3.65E-03	13
NO	GO:1901607	alpha-amino acid biosynthetic process	BP	4.13E-03	29
NO	GO:0046034	ATP metabolic process	BP	4.18E-03	26

NO	GO:1901136	carbohydrate derivative catabolic process	BP	4.65E-03	18
NO	GO:0072329	monocarboxylic acid catabolic process	BP	5.00E-03	15
NO	GO:0051495	positive regulation of cytoskeleton organization	BP	5.00E-03	15
NO	GO:0006733	oxidoreduction coenzyme metabolic process	BP	7.96E-03	21
NO	GO:0055088	lipid homeostasis	BP	8.13E-03	13
NO	GO:0006026	aminoglycan catabolic process	BP	8.13E-03	9
NO	GO:0006032	chitin catabolic process	BP	8.13E-03	9
NO	GO:0001731	formation of translation preinitiation complex	BP	8.13E-03	9
NO	GO:0044089	positive regulation of cellular component biogenesis	BP	8.70E-03	17
NO	GO:0009108	coenzyme biosynthetic process	BP	9.95E-03	22
NO	GO:0030170	pyridoxal phosphate binding	BP	4.71E-04	28
NO	GO:0016829	lyase activity	BP	5.56E-04	48
NO	GO:0051287	NAD binding	BP	6.96E-04	20
NO	GO:0004568	chitinase activity	BP	3.96E-03	9
NO	GO:0050662	coenzyme binding	BP	4.44E-03	55
NO	GO:0000062	fatty-acyl-CoA binding	BP	4.61E-03	14
NO	GO:0008483	transaminase activity	BP	7.20E-03	12
NO	GO:0052890	oxidoreductase activity, acting on the CH-CH group of donors, with a flavin as acceptor	BP	7.20E-03	12
NO	GO:1901681	sulfur compound binding	BP	9.49E-03	21
NO	GO:0044421	extracellular region part	BP	1.67E-05	65
NO	GO:0016282	eukaryotic 43S preinitiation complex	BP	2.65E-03	8
OO	GO:0033036	macromolecule localization	BP	1.42E-04	107
OO	GO:0006886	intracellular protein transport	BP	7.65E-03	57
OO	GO:0016050	vesicle organization	BP	6.34E-03	20
OO	GO:0009127	purine nucleoside monophosphate biosynthetic process	BP	5.19E-03	19
OO	GO:0009168	purine ribonucleoside monophosphate biosynthetic process	BP	5.19E-03	19
OO	GO:0005525	GTP binding	MF	2.02E-03	76
OO	GO:0032561	guanyl ribonucleotide binding	MF	1.53E-03	77
OO	GO:0019001	guanyl nucleotide binding	MF	1.53E-03	77
OO	GO:0044433	cytoplasmic vesicle part	CC	6.38E-05	13
OO	GO:0030118	clathrin coat	CC	6.98E-03	9
OO	GO:0043226	organelle	CC	3.16E-04	433

OO	GO:0016023	cytoplasmic membrane-bounded vesicle	CC	1.23E-04	22
OO	GO:0071013	catalytic step 2 spliceosome	CC	8.80E-03	12
OO	GO:0031410	cytoplasmic vesicle	CC	1.84E-04	22
OO	GO:0043229	intracellular organelle	CC	4.79E-04	424

Table S5 The Gene Ontology (GO) terms identified with significantly more abundant proteins in the offshore population at the offshore site (O→O) compared to the nearshore population (N→O) using metaGOmics (cutoff P < 0.01) (A), and those in the nearshore population at the offshore site (B) and BP=Biological process, MF= Molecular Function, and CC = Cellular Component of the GO categories.

(A)

GO Accession	GO Terms	GO Ca.	P-value	No. of Protein	%
GO:1901564	organonitrogen compound metabolic process	BP	2.68E-14	73	14.3%
GO:0043603	cellular amide metabolic process	BP	1.46E-12	45	8.8%
GO:0006518	peptide metabolic process	BP	2.82E-11	40	7.8%
GO:0043604	amide biosynthetic process	BP	3.99E-11	38	7.5%
GO:0044281	small molecule metabolic process	BP	8.11E-11	59	11.6%
GO:1901566	organonitrogen compound biosynthetic process	BP	2.60E-10	51	10.0%
GO:0043043	peptide biosynthetic process	BP	3.18E-10	35	6.9%
GO:0006412	translation	BP	6.09E-10	34	6.7%
GO:0019752	carboxylic acid metabolic process	BP	7.74E-08	36	7.1%
GO:0043436	oxoacid metabolic process	BP	2.65E-07	36	7.1%
GO:0006082	organic acid metabolic process	BP	3.11E-07	36	7.1%
GO:0006520	cellular amino acid metabolic process	BP	2.80E-06	25	4.9%
GO:0043038	amino acid activation	BP	6.07E-06	12	2.4%
GO:0043039	tRNA aminoacylation	BP	6.07E-06	12	2.4%
GO:0006418	tRNA aminoacylation for protein translation	BP	6.07E-06	12	2.4%
GO:0044710	single-organism metabolic process	BP	2.58E-05	103	20.2%
GO:0044271	cellular nitrogen compound biosynthetic process	BP	3.15E-05	50	9.8%
GO:0008152	metabolic process	BP	4.07E-05	232	45.5%
GO:1901576	organic substance biosynthetic process	BP	5.34E-04	65	12.7%
GO:0009058	biosynthetic process	BP	1.14E-03	67	13.1%
GO:0006807	nitrogen compound metabolic process	BP	3.10E-03	90	17.6%
GO:0044249	cellular biosynthetic process	BP	4.08E-03	61	12.0%
GO:0016875	ligase activity, forming carbon-oxygen bonds	MF	4.18E-06	12	2.4%
GO:0016876	ligase activity, forming aminoacyl-tRNA and related compounds	MF	4.18E-06	12	2.4%
GO:0004812	aminoacyl-tRNA ligase activity	MF	4.18E-06	12	2.4%

GO:0004177	aminopeptidase activity	MF	2.13E-03	8	1.6%
GO:0003735	structural constituent of ribosome	MF	6.80E-03	17	3.3%
GO:0005737	cytoplasm	CC	5.14E-15	115	22.5%
GO:0044444	cytoplasmic part	CC	4.63E-08	78	15.3%
GO:0022626	cytosolic ribosome	CC	3.60E-06	11	2.2%
GO:0044445	cytosolic part	CC	4.09E-05	13	2.5%
GO:0005829	cytosol	CC	4.32E-05	22	4.3%
GO:0005840	ribosome	CC	2.73E-04	16	3.1%
GO:0022625	cytosolic large ribosomal subunit	CC	6.55E-04	7	1.4%
GO:0044424	intracellular part	CC	7.21E-04	134	26.3%
GO:0005622	intracellular	CC	1.17E-03	149	29.2%
GO:0044391	ribosomal subunit	CC	1.37E-03	12	2.4%
GO:1990904	ribonucleoprotein complex	CC	1.65E-03	24	4.7%
GO:0030529	intracellular ribonucleoprotein complex	CC	1.65E-03	24	4.7%

(B)

GO Accession	GO Terms	GO Ca.	P-value	No. of Protein	%
GO:0005576	extracellular region	CC	4.33E-06	14	9.0%
GO:0044421	extracellular region part	CC	2.57E-04	10	6.5%

Table S6. Results of ANOVA and Tukey HSD Test on select GO terms, based on the sum of standardized NSAF values of the proteins belonging to the term. Results of Tukey HSD test are shown only for the ones with significant ANOVA results Significance codes: $P < 0.001$ (***) , $P = < 0.01$ (**), $P = < 0.05$ (*), $P = <0.1$ (.).

A. Biological Process terms

```
1. Intracellular protein transport

            Df Sum Sq Mean Sq F value Pr(>F)
Treatment    3  43999   14666   1.828   0.22
Residuals    8  64200    8025

2. Fatty acid beta oxidation using ACAD

            Df Sum Sq Mean Sq F value  Pr(>F)
Treatment    3  21600    7200   7.652 0.00977 **
Residuals    8   7528     941

  Tukey multiple comparisons of means
              diff        lwr        upr     p adj
O→N–N→N   87.08066  -22.79136 196.952672 0.0340538 *
N→O–N→N  -20.76059 -130.63260  89.111427 0.8395119
O→O–N→N   51.59391  -58.27810 161.465927 0.2442297
O→N–N→O -107.84124 -217.71326   2.030772 0.0111122 *
O→O–O→N  -35.48674 -145.35876  74.385272 0.5238253
O→O–N→O   72.35450  -37.51752 182.226516 0.0778260 .

3. Tricarboxylic acid cycle

            Df Sum Sq Mean Sq F value Pr(>F)
Treatment    3  36248   12083    2.09   0.18
Residuals    8  46252    5782


4. Purine ribonucleotide monophosphate biosynthetic process

            Df Sum Sq Mean Sq F value Pr(>F)
Treatment    3 174978   58326    4.33 0.0432 *
Residuals    8 107756   13470

 Tukey multiple comparisons of means
              diff       lwr      upr     p adj
O→N–N→N  236.06466 -179.6312 651.7605 0.1360807
N→O–N→N   36.45071 -379.2451 452.1466 0.9793198
O→O–N→N  -95.44398 -511.1398 320.2519 0.7499995
O→N–N→O -199.61395 -615.3098 216.0819 0.2297139
O→O–O→N -331.50864 -747.2045  84.1872 0.0330487 *
O→O–N→O -131.89469 -547.5905 283.8012 0.5372905

5. ATP metabolic process

            Df Sum Sq Mean Sq F value Pr(>F)
Treatment    3 422568  140856   1.989  0.194
Residuals    8 566539   70817
```

6. Arp2.3 complex mediated actin nucleation

```
            Df Sum Sq Mean Sq F value Pr(>F)
Treatment    3  16342    5447   1.858  0.215
Residuals    8  23450    2931
```

7. Nicotinamide nucleotide metabolic process

```
            Df Sum Sq Mean Sq F value Pr(>F)
Treatment    3 104727   34909   0.839  0.509
Residuals    8 332705   41588
```

8. tRNA aminoacylation for protein translation

```
            Df Sum Sq Mean Sq F value Pr(>F)
Treatment    3 157714   52571     3.8 0.0582 .
Residuals    8 110687   13836

 Tukey multiple comparisons of means
              diff       lwr      upr     p adj
O→N-N→N  154.22823 -267.0827 575.5391 0.4270946
N→O-N→N   44.34379 -376.9671 465.6547 0.9653726
O→O-N→N  297.02184 -124.2890 718.3327 0.0583582 .
O→N-N→O -109.88444 -531.1953 311.4264 0.6749050
O→O-O→N  142.79361 -278.5173 564.1045 0.4868867
O→O-N→O  252.67806 -168.6328 673.9889 0.1119362
```

9. Oxidation reduction process

```
            Df Sum Sq Mean Sq F value Pr(>F)
Treatment    3 360099  120033   1.653  0.253
Residuals    8 581023   72628
```

10. Translation

```
            Df  Sum Sq Mean Sq F value Pr(>F)
Treatment    3 4064599 1354866   2.805  0.108
Residuals    8 3864558  483070
```

11. Cellular amino acid metabolic process

```
            Df  Sum Sq Mean Sq F value  Pr(>F)
Treatment    3 1025423  341808    9.47 0.00521 **
Residuals    8  288758   36095

 Tukey multiple comparisons of means
             diff         lwr       upr     p adj
O→N-N→N  480.3480  -200.14187 1160.8378 0.0580372 .
N→O-N→N  113.9304  -566.55948  794.4202 0.8806434
O→O-N→N  734.5202    54.03030 1415.0100 0.0064157 **
O→N-N→O -366.4176 -1046.90747  314.0722 0.1626623
O→O-O→N  254.1722  -426.31768  934.6620 0.4114674
O→O-N→O  620.5898   -59.90006 1301.0796 0.0166395 *
```

12. Cellular oxidant detoxification

```
            Df Sum Sq Mean Sq F value Pr(>F)
Treatment    3  46796   15599   4.599 0.0375 *
Residuals    8  27132    3392

 Tukey multiple comparisons of means
               diff        lwr       upr     p adj
O→N–N→N -131.543874 -340.13662  77.04887 0.0925100 .
N→O–N→N  -21.006700 -229.59945 187.58605 0.9693972
O→O–N→N -137.342967 -345.93571  71.24978 0.0778781 .
O→N–N→O  110.537174  -98.05557 319.12992 0.1712375
O→O–O→N   -5.799092 -214.39184 202.79365 0.9992950
O→O–N→O -116.336267 -324.92901  92.25648 0.1447643
```

13. Coenzyme biosynthetic process

```
            Df Sum Sq Mean Sq F value Pr(>F)
Treatment    3  17953    5984   2.375  0.146
Residuals    8  20159    2520
```

14. Oxidoreduction coenzyme metabolic process

```
            Df Sum Sq Mean Sq F value Pr(>F)
Treatment    3  99000   33000   0.792  0.532
Residuals    8 333279   41660
```

15. Chitin catabolic process

```
            Df Sum Sq Mean Sq F value Pr(>F)
Treatment    3   1708   569.4   0.709  0.573
Residuals    8   6422   802.8
```

16. Hexose metabolic process

```
            Df Sum Sq Mean Sq F value Pr(>F)
Treatment    3  66802   22267   0.992  0.444
Residuals    8 179568   22446
```

17. Lipid homeostasis

```
            Df Sum Sq Mean Sq F value Pr(>F)
Treatment    3  20519    6840   7.085 0.0122 *
Residuals    8   7723     965

 Tukey multiple comparisons of means
              diff        lwr       upr     p adj
O→N–N→N   82.48250  -28.80861 193.77361 0.0466801 *
N→O–N→N  -21.02863 -132.31975  90.26248 0.8395137
O→O–N→N   54.20854  -57.08257 165.49966 0.2206806
O→N–N→O -103.51113 -214.80225   7.77998 0.0149627 *
O→O–O→N  -28.27396 -139.56507  83.01716 0.6914214
O→O–N→O   75.23718  -36.05394 186.52829 0.0698235 .
```

18. Protein folding

```
            Df  Sum Sq Mean Sq F value Pr(>F)
Treatment    3   16736    5579   0.042  0.988
Residuals    8 1058748  132344
```

19. Ribonucleoprotein complex assembly

```
            Df Sum Sq Mean Sq F value Pr(>F)
Treatment    3  49125   16375   1.718   0.24
Residuals    8  76261    9533
```

20. Dicarboxylic acid metabolic process

```
            Df Sum Sq Mean Sq F value Pr(>F)
Treatment    3  31063   10354    3.97 0.0528 .
Residuals    8  20863    2608

  Tukey multiple comparisons of means
              diff        lwr       upr     p adj
O→N–N→N   68.07492 -114.83575 250.98558 0.4142487
N→O–N→N  113.59993  -69.31073 296.51060 0.0981410 .
O→O–N→N  -10.78210 -193.69277 172.12857 0.9934553
O→N–N→O   45.52501 -137.38565 228.43568 0.7039609
O→O–O→N  -78.85702 -261.76768 104.05365 0.3033466
O→O–N→O -124.38203 -307.29270  58.52863 0.0681239 .
```

21. Alpha amino acid biosynthetic process

```
            Df Sum Sq Mean Sq F value  Pr(>F)
Treatment    3 139687   46562   7.596 0.00998 **
Residuals    8  49041    6130

  Tukey multiple comparisons of means
              diff        lwr      upr     p adj
O→N–N→N  206.30079  -74.13671 486.7383 0.0482908 *
N→O–N→N   41.97989 -238.45761 322.4174 0.9102921
O→O–N→N  257.06949  -23.36801 537.5070 0.0161864 *
O→N–N→O -164.32090 -444.75840 116.1166 0.1218409
O→O–O→N   50.76870 -229.66880 331.2062 0.8552430
O→O–N→O  215.08960  -65.34790 495.5271 0.0398235 *
```

22. Small molecule biosynthetic process

```
            Df Sum Sq Mean Sq F value Pr(>F)
Treatment    3 110233   36744   1.561  0.273
Residuals    8 188350   23544
```

23. Carboxylic acid catabolic process

```
            Df Sum Sq Mean Sq F value Pr(>F)
Treatment    3  27840    9280   2.409  0.142
Residuals    8  30812    3852
```

```
24. Vesicle organization
            Df Sum Sq Mean Sq F value Pr(>F)
Treatment    3  83257   27752   5.858 0.0204 *
Residuals    8  37898    4737

 Tukey multiple comparisons of means
             diff        lwr      upr     p adj
O→N-N→N -12.22093 -258.74651 234.3046 0.9960686
N→O-N→N -44.42170 -290.94728 202.1039 0.8568778
O→O-N→N 169.79523  -76.73034 416.3208 0.0645332 .
O→N-N→O -32.20077 -278.72635 214.3248 0.9374186
O→O-O→N 182.01616  -64.50941 428.5417 0.0474974 *
O→O-N→O 214.21693  -32.30864 460.7425 0.0214729 *

25. Translational initiation

            Df Sum Sq Mean Sq F value Pr(>F)
Treatment    3 367454  122485   1.858  0.215
Residuals    8 527333   65917

26. Formation of translation preinitiation complex
            Df Sum Sq Mean Sq F value Pr(>F)
Treatment    3  622.3  207.44   4.068 0.0499 *
Residuals    8  407.9   50.99

 Tukey multiple comparisons of means
              diff        lwr      upr     p adj
O→N-N→N 13.4729778 -12.103215 39.04917 0.1744922
N→O-N→N 12.6351111 -12.941082 38.21130 0.2119123
O→O-N→N 19.8672000  -5.708993 45.44339 0.0375010 *
O→N-N→O -0.8378667 -26.414060 24.73833 0.9988498
O→O-O→N  6.3942222 -19.181971 31.97042 0.7012590
O→O-N→O  7.2320889 -18.344104 32.80828 0.6209750
```

B. Molecular Function and Cellular Component terms

```
1. Aminoacyl-tRNA ligase activity

            Df Sum Sq Mean Sq F value Pr(>F)
Treatment    3 157714   52571     3.8 0.0582 .
Residuals    8 110687   13836

  Tukey multiple comparisons of means
              diff       lwr      upr     p adj
O→N-N→N  154.22823 -267.0827 575.5391 0.4270946
N→O-N→N   44.34379 -376.9671 465.6547 0.9653726
O→O-N→N  297.02184 -124.2890 718.3327 0.0583582 .
O→N-N→O -109.88444 -531.1953 311.4264 0.6749050
O→O-O→N  142.79361 -278.5173 564.1045 0.4868867
O→O-N→O  252.67806 -168.6328 673.9889 0.1119362
```

2. Chitinase activity

```
            Df Sum Sq Mean Sq F value Pr(>F)
Treatment    3   1670   556.7   0.649  0.605
Residuals    8   6857   857.1
```

3. Serine-type endopeptidase inhibitor activity

```
            Df Sum Sq Mean Sq F value Pr(>F)
Treatment    3  80765   26922   5.763 0.0213 *
Residuals    8  37374    4672

  Tukey multiple comparisons of means
              diff        lwr      upr     p adj
O→N-N→N   58.86942 -185.94526 303.6841 0.7242563
N→O-N→N  -46.37221 -291.18689 198.4425 0.8385676
O→O-N→N  172.91650  -71.89818 417.7312 0.0578829 .
O→N-N→O -105.24163 -350.05631 139.5731 0.3054270
O→O-O→N  114.04708 -130.76760 358.8618 0.2495148
O→O-N→O  219.28871  -25.52597 464.1034 0.0183126 *
```

4. Fatty-acyl-CoA binding

```
            Df Sum Sq Mean Sq F value  Pr(>F)
Treatment    3  23847    7949   8.245 0.00787 **
Residuals    8   7713     964

  Tukey multiple comparisons of means
              diff        lwr         upr     p adj
O→N-N→N   92.06956  -19.14384 203.2829485 0.0274833 *
N→O-N→N  -20.11988 -131.33327  91.0935152 0.8554793
O→O-N→N   56.49809  -54.71530 167.7114818 0.1951296
O→N-N→O -112.18943 -223.40283  -0.9760404 0.0095142 **
O→O-O→N  -35.57147 -146.78486  75.6419263 0.5312176
O→O-N→O   76.61797  -34.59543 187.8313596 0.0644635 **
```

5. GTP binding

```
            Df  Sum Sq Mean Sq F value Pr(>F)
Treatment    3  368033  122678   0.743  0.556
Residuals    8 1320028  165004
```

6. Hydro-lyase activity

```
            Df Sum Sq Mean Sq F value Pr(>F)
Treatment    3  36161   12054   2.293  0.155
Residuals    8  42051    5256
```

7. Intramolecular transferase activity -Phosphotransferases

```
            Df Sum Sq Mean Sq F value Pr(>F)
Treatment    3    371   123.5   0.211  0.886
Residuals    8   4675   584.4
```

8. NAD binding

```
            Df Sum Sq Mean Sq F value Pr(>F)
Treatment    3 111122   37041   1.726  0.239
Residuals    8 171668   21458
```

9. Oxidoreductase activity acting on the CH-CH group of donors with a flavin as acceptor

```
            Df Sum Sq Mean Sq F value  Pr(>F)
Treatment    3  21600    7200   7.652 0.00977 **
Residuals    8   7528     941

  Tukey multiple comparisons of means
              diff        lwr        upr     p adj
O→N-N→N   87.08066  -22.79136 196.952672 0.0340538 *
N→O-N→N  -20.76059 -130.63260  89.111427 0.8395119
O→O-N→N   51.59391  -58.27810 161.465927 0.2442297
O→N-N→O -107.84124 -217.71326   2.030772 0.0111122 *
O→O-O→N  -35.48674 -145.35876  74.385272 0.5238253
O→O-N→O   72.35450  -37.51752 182.226516 0.0778260 .
```

10. Pyridoxal phosphate binding

```
            Df Sum Sq Mean Sq F value Pr(>F)
Treatment    3  72467   24156   12.64 0.0021 **
Residuals    8  15289    1911

  Tukey multiple comparisons of means
              diff         lwr      upr     p adj
O→N-N→N  191.27434   34.693574 347.8551 0.0030106 **
N→O-N→N   57.16728  -99.413485 213.7480 0.4291559
O→O-N→N  163.44598    6.865215 320.0267 0.0078118 **
O→N-N→O -134.10706 -290.687822  22.4737 0.0231359 *
O→O-O→N  -27.82836 -184.409122 128.7524 0.8616149
O→O-N→O  106.27870  -50.302063 262.8595 0.0686615 .
```

11. Transaminase Activity

```
            Df Sum Sq Mean Sq F value Pr(>F)
Treatment    3  36162   12054   10.01 0.0044 **
Residuals    8   9635    1204

  Tukey multiple comparisons of means
               diff         lwr        upr     p adj
O→N-N→N  115.985581   -8.316007 240.287170 0.0147025 *
N→O-N→N   -4.738389 -129.039978 119.563200 0.9981946
O→O-N→N   97.127311  -27.174278 221.428900 0.0364604 *
O→N-N→O -120.723970 -245.025559   3.577619 0.0117888 *
O→O-O→N  -18.858270 -143.159859 105.443319 0.9071238
O→O-N→O  101.865700  -22.435889 226.167289 0.0289093 *
```

12. Translation initiation factor activity

```
            Df Sum Sq Mean Sq F value Pr(>F)
Treatment    3   6236  2078.7   3.976 0.0526 .
Residuals    8   4183   522.9

  Tukey multiple comparisons of means
             diff       lwr       upr     p adj
O→N-N→N 14.507985 -67.39352  96.40949 0.8627303
N→O-N→N 11.144678 -70.75683  93.04619 0.9301864
O→O-N→N 59.715689 -22.18582 141.61720 0.0502741 .
O→N-N→O-3.363307 -85.26482  78.53820 0.9977481
O→O-O→N 45.207704 -36.69380 127.10921 0.1499005
O→O-N→O 48.571011 -33.33050 130.47252 0.1166457
```

13. Catalytic step 2 spliceosome

```
            Df Sum Sq Mean Sq F value Pr(>F)
Treatment    3   6092  2030.6   2.075  0.182
Residuals    8   7829   978.6
```

14. Clathrin coat

```
            Df Sum Sq Mean Sq F value Pr(>F)
Treatment    3  13640    4547   2.413  0.142
Residuals    8  15072    1884
```

15. Cytosolic large ribosomal subunit

```
            Df Sum Sq Mean Sq F value Pr(>F)
Treatment    3 427596  142532   2.125  0.175
Residuals    8 536482   67060
```

16. Endosome

```
            Df Sum Sq Mean Sq F value  Pr(>F)
Treatment    3  75819   25273   7.642 0.00981 **
Residuals    8  26456    3307

  Tukey multiple comparisons of means
              diff         lwr      upr     p adj
O→N-N→N   48.43543 -157.541539 254.4124 0.7369189
N→O-N→N  -52.81124 -258.788216 153.1657 0.6857159
O→O-N→N  162.42949  -43.547483 368.4065 0.0348918 *
O→N-N→O -101.24668 -307.223650 104.7303 0.2150078
O→O-O→N  113.99406  -91.982916 319.9710 0.1485838
O→O-N→O  215.24073    9.263761 421.2177 0.0077627 **
```

17. Eukaryotic translation initiation factor 3 complex

```
            Df Sum Sq Mean Sq F value Pr(>F)
Treatment    3  173.8   57.94   1.229  0.361
Residuals    8  377.0   47.13
```

18. Extracellular exosome

```
            Df Sum Sq Mean Sq F value Pr(>F)
Treatment    3   6379    2126   0.963  0.456
Residuals    8  17663    2208
```

19. Extracellular region part

```
            Df Sum Sq Mean Sq F value Pr(>F)
Treatment    3   4712    1571   0.311  0.817
Residuals    8  40438    5055
```

20. mitochondrion

```
            Df Sum Sq Mean Sq F value  Pr(>F)
Treatment    3 753591  251197   12.03 0.00247 **
Residuals    8 167072   20884
```

```
  Tukey multiple comparisons of means
              diff        lwr        upr     p adj
O→N-N→N  458.94609  -58.66891  976.56110 0.0193245 *
N→O-N→N   37.69248 -479.92253  555.30748 0.9878799
O→O-N→N  567.80902   50.19402 1085.42403 0.0058274 **
O→N-N→O -421.25361 -938.86862   96.36139 0.0299201 *
O→O-O→N  108.86293 -408.75207  626.47793 0.7940571
O→O-N→O  530.11654   12.50154 1047.73155 0.0087232 **
```

21. Oxidoreductase complex

```
            Df Sum Sq Mean Sq F value Pr(>F)
Treatment    3  14165    4722   1.015  0.435
Residuals    8  37206    4651
```

22. Proteasome regulatory particle - base subcomplex

```
            Df Sum Sq Mean Sq F value Pr(>F)
Treatment    3   4831  1610.2    5.85 0.0205 *
Residuals    8   2202   275.2
```

```
  Tukey multiple comparisons of means
              diff        lwr       upr     p adj
O→N-N→N  51.755041  -7.666599 111.17668 0.0212136 *
N→O-N→N  23.361778 -36.059862  82.78342 0.3720075
O→O-N→N  43.895256 -15.526384 103.31690 0.0473855 *
O→N-N→O -28.393263 -87.814903  31.02838 0.2328847
O→O-O→N  -7.859785 -67.281425  51.56185 0.9352725
O→O-N→O  20.533478 -38.888162  79.95512 0.4718991
```

23. Transport vesicle membrane

```
            Df Sum Sq Mean Sq F value Pr(>F)
Treatment    3   9987    3329   4.934 0.0316 *
Residuals    8   5398     675
```

```
  Tukey multiple comparisons of means
             diff        lwr       upr     p adj
O→N-N→N  32.77486  -60.26553 125.81524 0.4569728
N→O-N→N -46.25353 -139.29392  46.78685 0.2080707
O→O-N→N -19.81356 -112.85394  73.22683 0.7881738
O→N-N→O -79.02839 -172.06878  14.01199 0.0241389 *
O→O-O→N -52.58841 -145.62880  40.45197 0.1383033
O→O-N→O  26.43998  -66.60041 119.48036 0.6175099
```

Table S7. Comparison of detoxification protein abundance between nearshore and offshore coral populations. The average standardized NSAF values of detoxification proteins with and without two peroxiredoxins (m.9595 and m.6147), and corresponding ANOVA results are shown.

Treatments	N→N	N→O	Ave. Nearshore	O→N	O→O	Ave. Offshore	F value (P-value)
All 27 proteins	1484.5	1463.5		1352.9	1347.1		
			1474.0			1350.0	16.55** (0.00226)
2 Prxs	977.0	1023.6		722.1	687.2		
			1000.3			704.6	22.63*** (0.00077)
w/o 2 Prxs	507.4	439.8		630.9	660.0		
			473.6			645.4	5.424* (0.0421)

Table S8. Summary of significantly differentially expressed proteins between samples

Comparison	N→N *vs.* N→O	N→N *vs.* O→N	O→N *vs.* O→O	N→O *vs.* O→O	N→N *vs.* O→O
No. of differentially expressed proteins	135 (87, 48)	414 (138, 276)	440 (172, 268)	665 (155, 510)	644 (181, 463)
No. of unique proteins	573 (231, 342)	925 (402, 523)	976 (642, 334)	1019 (656, 363)	967 (577, 390)

Table S8. Detoxification protein summary

	N→O	N→N	O→N	O→O	ANOVA Tukey HSD
No. of proteins identified	20	23	27	20	
Total NSAF	1463.5±42.8	1484.5±74.9	1352.9±64.6	1347.1±44.0	*P* = 0.0375* ns
Total NSAF without m. 17739 &m.9595	439.8±86.7	507.4±148.3	630.9±127.9	650.0±89.5	*P* = 0.251 ns
NSAF of m.17739 & m. 9595	1023.6±129.6	977.0±223.2	722.05±192.5	687.15±133.5	*P* = 0.0159* 6, (3,4 marginal)
No. of proteins with significant fold change between N→N & O→N		1	4		
No. of proteins with positive fold change between N→N & O→N		11	16		

Table S9. DNA sequence accession numbers for the *P. lobata* colonies used in the experiment

Source location	Sample ID	Marker	GenBank Accession No.
Nearshore	N1	H2	KY502354
Nearshore	N2	H2	KY502357
Nearshore	N3	H2	KY502358
Nearshore	N4	H2	KY502362
Nearshore	N5	H2	KY502364
Offshore	O1	H2	KY502366
Offshore	O2	H2	KY502370
Offshore	O3	H2	KY502369
Offshore	O4	H2	KY502368
Offshore	O5	H2	MF629151